6G-REFERENCE

D1.1

6G-REFERENCE Distributed Radio Specification

WP1

System Analysis and Design

Work package	WP1
Task	T1.1, T1.2, T1.3
Due date	31-08-2024
Submission date	30-08-2024
Deliverable lead	Ericsson
Version	v1.2
Authors	Pallavi Paliwal (EAB), Stefan Andersson (EAB), Xavier Artiga (CTTC), Ignacio Llamas (CTTC), Zabdiel Brito (CTTC), Guido Luzi (CTTC), Riccardo Palamà (CTTC), Dominique Morche (CEA), Erwin Hardeveld (UT), Robin Lohuis (UT), Harijot Bindra (UT), Eric Klumperink (UT), Hua Wang (ETHZ), Christoph Studer (ETHZ), Yi Wang (UB), Marc Bauduin (IMEC)
Reviewers	Dominique Morche (CEA), Hua Wang (ETHZ), Eric Klumperink (UT)

Funded by the European Union

Abstract

This deliverable collects outputs of the system level study of the 6G-REFERENCE project. It describes an open distributed radio architecture supporting multiple 6G functionalities for communication, sensing and synchronization. It discusses use cases and applications, derives system-level functional requirements focusing on the integrated fronthaul- and access-link, sensing and timing synchronization. The document also discusses and forms a baseline for initial high-level building block level specifications.

Keywords

6G Communication systems, Distributed MIMO (D-MIMO), Coherent Joint Transmission, Full Duplex, Beamforming, Integrated Communication and Sensing, Radar, Phased Arrays, Reconfigurable Intelligent Surfaces (RIS), Frequency synchronization, Over the air (OTA) synchronization, Time Synchronization, UTC time.

Document revision history

Version	Date	Description of change	Authors
V0.1	30-06-2024	1st version / template	Antonis Sapountzis
V1	28-08-2024	Complete Version for review	See first page
V1.1	29-08-2024	Reviewed version	See first page
V1.2	30-08-2024	Final version submitted	Stefan/Pallavi

Disclaimer

Copyright notice

Document information

Nature of the deliverable **R – Document, Report**		
Dissemination level		
PU	Public, fully open. e.g., website	✓
CL	Classified information as referred to in Commission Decision 2001/844/EC	
SEN	Confidential to 6G-REFERENCE project and Commission Services	

* **Deliverable types**:
R: document, report (excluding periodic and final reports).
DEM: demonstrator, pilot, prototype, plan designs.
DEC: websites, patent filings, press and media actions, videos, etc.
OTHER: software, technical diagrams, etc.

Table of contents

List of figures

List of tables

Acronyms and definitions

3GPP	3rd Generation Partnership Project
AoA	Angle of Arrival
ACLR	Adjacent Channel Leakage Ratio
ADC	Analog to Digital Converter
AGV	Automated Guided Vehicle
AM	Amplitude Modulation
AMR	Autonomous Mobile Robots
AP	Access Point
BW	Bandwidth, usually the communication channel bandwidth
CJT	Coherent Joint Transmission
CP	Cyclic Prefix
CU	Central Processing Unit
D-MIMO	Distributed MIMO
DU	Distributed Processing Unit
EESS	Earth Exploration-Satellite Services
FA	Filtering by Aliasing
FDA	Frequency Diversity Array
FMA	Frequency Modulated Array
FoV	Field of View
FTA	Frequency Translation by Aliasing
GPS	Global Positioning System
GNSS	Global Navigation Satellite System
IF	Intermediate Frequency
IL	Insertion Loss
IMT	International Mobile Telecommunications
ITU	International Telecommunications Union
KPI	Key Performance Indicator

Funded by the European Union

LLC	Low Latency Communication
LoS	Line of Sight
NGNM	Next Generation Mobile Networks Alliance
NTN	Non-Terrestrial Network
OTA	Over the air
PAPR	Peak to Average Power Ratio
PL	Path Loss
PM	Phase Modulation
PRF	Pulse Repetition Frequency
PTP	Precision Time Protocol
RIS	Reconfigurable Intelligent Surface
RU	Radio Unit
SCS	Sub Carrier Spacing
SINR	Signal-to-Interference and Noise Ratio
SNR	Signal to Noise Ratio
TDD	Time Division Duplex
TMA	Time Modulated Array
TSN	Time Sensitive Networks
UE	User Equipment
UTC	Universal Coordinated Time
WP	Work Package
XR	eXtended Reality: umbrella term for augmented reality (AR), virtual reality (VR) en mixed reality (MR)

Funded by the European Union

1. Executive summary

This report summarizes initial system study work done in the 6G-Reference project to convert rather general ideas on useful hardware capabilities/enablers for future 6G systems to concrete system and block level KPIs for concrete use-case scenarios. We evaluated various proposed 6G use-case scenarios related to communication and sensing, with special focus on proposals of project HEXA-X-II. We selected three best fitting use cases: 1) An urban square communication scenario with densely distributed RUs (D-MIMO deployment) for cell-free uniform coverage, while incorporating basic sensing capabilities; 2) A factory hall scenario with more a regular deployment grid supporting communication but also higher performance sensing capabilities; 3) A timing focussed use scenario (Time Sensitive Network) with special focus on providing high performance time stamping to UTC. We selected the 14.8-15.35GHz cm-wave band as target band with 50-400MHz channel bandwidth and defined a deployment grid with about 25m spacing between access points. Requirements on communication and sensing were defined in quite some detail linked to the use-case scenarios. The hardware enablers focused on in this project are (1) a full-duplex AP-AP link with higher modulation scheme than the access link allowing the RU to satisfy needed fronthaul capacity, while also integrating the UE-AP access link, (2) an RF frequency synthesizer for AP-AP links synchronizing over the air and aligning coherently with low timing error to allow for coherent joint transmission (3) waveform/hardware co-design supporting integrated radar sensing in line with 3GPP Rel-19, (4) Localization support by using high-resolution FMA, (5) concurrent multi-beam Tx and Rx re-using beamforming hardware in a TMA, (6) Phased Array antenna panel designs supporting functionalities, (7) RIS based beamforming performance improvement. The initial key KPIs for the blocks were identified and some initial system level feasibility estimates were made. This will be further worked out in the coming year.

2. Introduction

The overall aim of 6G-REFERENCE is to develop hardware enablers constituting a reference design of distributed radios for a cell-free joint communication and sensing system operating in the Frequency Range 3 (FR3) range, i.e., at centimetric waves (cm-waves). Such a system will be able to cope with the following key goals of future 6G systems:

- User centric systems
- Increased spectral efficiency through efficient frequency reuse, improved beamforming resolution and interference management
- Use of new spectrum to deal with increased capacity requirements
- Physical, digital and human world interconnectivity
- Communications, computation and sensing edge-cloud continuum
- Sustainability

More specifically, cell-free systems are inherently user centric, since a subset of distributed nodes, i.e., radio units (RU) are selected to coherently serve a given user, but the selected set changes from user-to-user or with the user location. In this way, it can be ensured that each user is served by the best (typically the closer) set of RUs, thus providing the best service to each user. Moreover, the coherent transmission from multiple RUs allows improving the beamforming resolution, thus properly handling the multi-user interference, and enabling aggressive frequency reuse schemes resulting in a net system capacity increase. The larger the number of RUs cooperating, the better beamforming performance. Therefore, it is envisaged that in very high population density areas, the cell-free concept will translate to a massive deployment of distributed RUs, ensuring multi-RU coverage in every corner. This RU densification will also reduce the distance between the RU and the users, reducing the path loss and enabling significant power consumption and complexity savings in the RUs, making the system scalable and sustainable. Besides, it will also permit reducing the RU form factors, resulting in better aesthetics and enabling the possibility of camouflaging them with urban furniture. Since every RU will have limited but still some processing capabilities, this distributed massive deployment will contribute to form a communication and computing edge-cloud continuum, in which the network will have the possibility to efficiently manage all communication and computational resources to provide the most efficient service to all users in the area.

Joint communications and sensing will permit bridging the physical, digital and human world offering a radically new user experience that will represent a change of paradigm in how communication devices impact on human lives. Distributed sensing across the deployment area and accurate localization of users within it, will permit monitoring the surroundings of the users and providing them situational awareness for an uncountable number of applications, realizing the internet of senses.

Finally, the use of FR3 brings new and improved opportunities since cm-waves provide the best balance between sub-6GHz and mm-wave. Their principal benefits are that they can allocate similarly large channel bandwidths as with mm-waves, but they experience less pathloss, so the complexity, power consumption and cost with respect to mm-wave can be significantly reduced, leveraging to more sustainable systems. Besides, they offer a channel sparsity lower than mm-waves but still significantly higher than sub-6GHz, which translates to less exposure to multipath effects.

Note however, that the implementation of the described system faces multiple open research challenges. Cell-free and distributed multi-antenna (D-MIMO) wireless systems have received significant attention from academia and industry in recent years (Ngo *et al.*, 2017; Interdonato *et al.*, 2019) and are widely believed to be a core technology in upcoming wireless standards. Past research has extensively focused on mostly the theory and algorithm levels, such as analysing spectral efficiency or devising power allocation, beamforming, and user scheduling schemes. However, despite the necessity of accurate time- and frequency-synchronization to support coherent beamforming and coordinated transmission in both the uplink and downlink, such critical aspects have been largely ignored in the open literature, with a few exceptions (Ruffini *et al.*, 2021). In addition, the envisioned massive densification of cooperating RUs for 6G, will pose new challenges for providing front/back-haul access to all nodes in a low-latency, concurrent, and synchronized manner. This is even more challenging if RUs lack cabled access, as is very much desired for flexible and sustainable deployment scenarios in spaces with limited existing infrastructure. Joint communication and sensing pose new challenges in the hardware itself since it must be able to deal with very distinct requirements coming from the two worlds. The use of FR3 besides being an opportunity, requires increased frequency selectivity due to the use of the spectrum by other systems like Fixed Satellite Services. Last but not least, all these capabilities should be achieved in an ecologically and economically sustainable manner, which translates to low cost, low power, distributed nodes with small form factors, also for aesthetics reasons. Summarizing, 6G-REFERENCE technological developments must allow de-risking the implementation of distributed cell-free joint communication and sensing system at FR3 by addressing the following fundamental system level challenges:

1. Coherent cooperative transmission to user terminals from a group of distributed RUs and efficient over-the-air (OTA) fronthaul data distribution amongst them.
2. Accurate Over-the-Air Synchronization (OAS) of distributed RUs.
3. Accurate sensing and localization capabilities using the same RU hardware platform.
4. Increased selectivity in frequency and spatial dimension, to co-exist with other services in FR3 bands.
5. Sustainability in economic and ecologic sense

The aim of this deliverable is to translate these system level challenges to block (i.e., circuit/antenna/algorithm) level specifications that will drive the research throughout the project. For this, we follow a top-down approach that includes: the identification of relevant 6G use cases, deployment scenarios and targeted KPIs; the identification of a high-level system and RU architectures; the in-depth analysis of deployment scenarios with especial focus on the derivation of specifications for the communications, sensing synchronization and frequency selectivity system capabilities; and an initial derivation of block-level specifications.

3. Use cases, deployment scenarios and architecture

This chapter first analyses the relevant 6G use cases and deployment scenarios proposed by main industrial associations and standardization bodies, which have been already discussed in initial 3GPP steps towards 6G. It then proposes three 6G-REFERENCE baseline scenarios and a baseline system and RU architecture.

3.1. Revision of proposed 6G use cases

6G use cases still have not been agreed in the 3GPP framework. Indeed, in May 2024 the 3GPP Stage-1 workshop on IMT-2030 (i.e. 6G) use cases (3GPP, 2024a) took place, which represented a sort of kick off for 6G activities within the 3GPP, with the first Study Item in the SA I Working Group planned for September 2024. In the workshop, industrial associations (GSMA, NGMN, 5G-AA, 5G-ACIA, 5G-MAG, GSOA, TCCA and WBA), regional research alliances (from Japan, China, Korea, India, North America and Europe) and standardization bodies (ITU-R, 3GPP) shared their visions on 6G use cases. Remarkably, a common message from industrial associations, like GSMA, NGMN, 5G-AA and 5C-ACIA was the suggestion to slow down the pace on the 6G development by the acknowledgment that 5G has still a long way to go and that most 5G use cases will still be relevant in 6G and will benefit from improved radio and network performance. ITU-R already gathered that vision in its definition of use cases for IMT-2030 (ITU, 2023), which was cited by a large portion of the participants in the workshop, and thus can be seen as the most agreed vision on 6G use cases today. As shown in Figure 1, it considers three usage scenarios that just push the performance limits of main 5G use cases and three new 6G ones. In this way, enhanced Mobile Broadband evolves to Immersive Communication, Ultra-Reliable Low-Latency Communication (LLC) to Hyper-Reliable Low-Latency Communication and massive Machine Type Communication to Massive Communication. They are then complemented with native integration of Sensing, AI and the non-terrestrial network (NTN) components to achieve Ubiquitous connectivity.

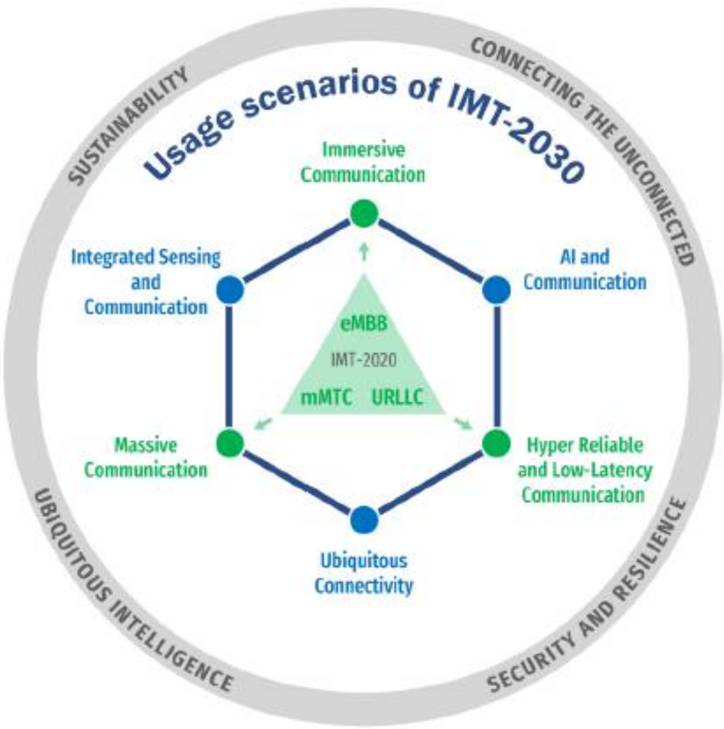

Figure 1. ITU-R usage scenarios for IMT-2030 (ITU, 2023).

Clearly, the described 6G-REFERENCE concept introduced in Section 2, aligns best with **the Immersive Communications** and **Integrated Sensing and Communication** usages. The former considers urban or rural hotspots with enhanced spectrum efficiency capable of consistently providing immersive XR, remote multi-sensory telepresence, and/or holographic communication services. Remarkably, it requires time-synchronized transmission of video, audio and/or environmental data. The latter, considers wide area multi-dimensional sensing for assisted navigation, activity detection and movement tracking, environmental monitoring and provision of sensing data for AI, XR, and digital twin applications.

Let us now consider the proposed 6G use cases by NGMN (NGMN, 2022), which had a key role in the definition of 5G use cases. Although using a different classification with respect to ITU-R, as depicted in Figure 2, many commonalities can be observed. Immersive communications have a key role in enhanced human communications, machine communications and services like smart industry, or digital healthcare can be related to Hyper-Reliable LLC and coverage expansion is related to ubiquitous communications. Moreover, NGMN explicitly acknowledges that integrated sensing and communications and AI will be required in multiple use cases to satisfy the requirements. Regarding the relevance to 6G-REFERENCE concept, let us highlight the foreseen **increased data rates for enhanced human communication, time synchronization requirements in enhanced machine communication, accurate 3D-localization in multiple services and integrated sensing and communications for services exploiting situational awareness information.**

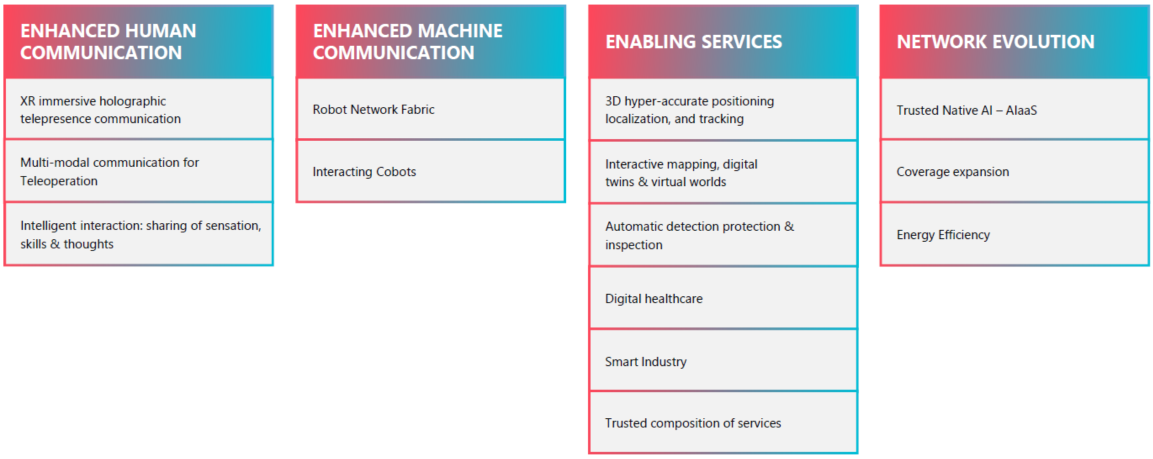

Figure 2. NGMN use cases (NGMN, 2022).

Finally, let us review the European vision on 6G use cases, which comes mainly from the outputs of SNS phase I projects and in particular, from Hexa-X-II (Hexa-X-II, 2023). As shown in Figure 3, a new different classification but again with many commonalities is proposed.

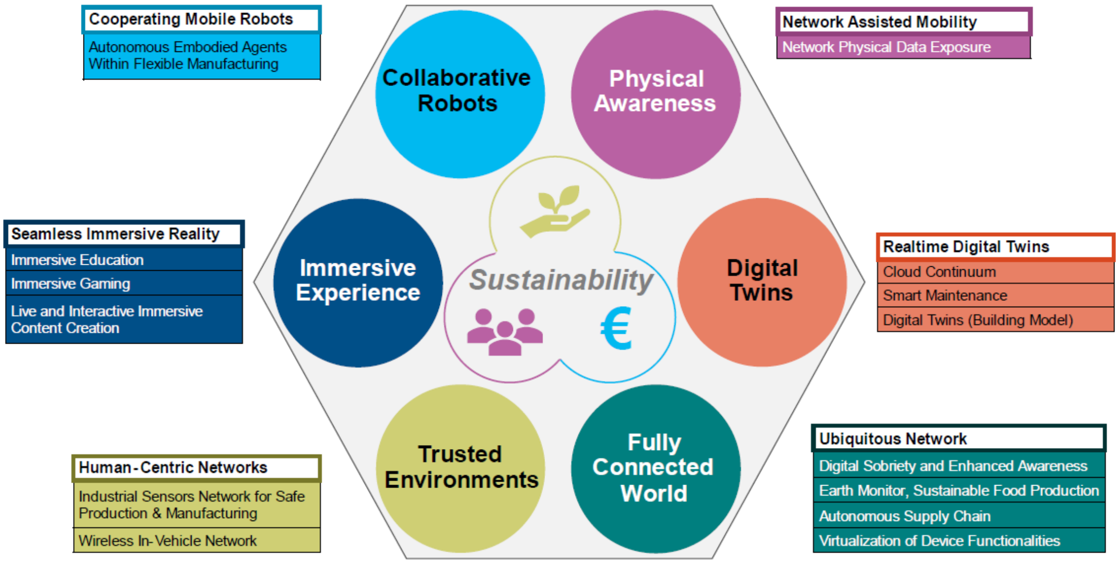

Figure 3. 6G use cases from Hexa-X II project (Hexa-X-II, 2023).

Let us now identify the use cases relevant to the 6G-REFERENCE concept. First, similarly to the Immersive communication usage form ITU-R, the **Immersive experience "on the go"** considers a wide area deployment in urban/sub-urban environments, with a high-density deployment of small cells providing high bandwidth and high area traffic capacity. It requires accurate positioning and integrated sensing and communications or sensor fusion (i.e., information extracted from embedded sensors) to provide an immersive experience. Second, **Collaborative robots** may consider large indoor deployments with scarcity of line-of-sight links, thus requiring denser deployments of pico/femto cells. Sensing and positioning capabilities integrated into the radio interface are required for robot control and coordination. In addition, one of the considered types of robots/machines, are those with a high level of autonomy, reliant on sensor data exchange and AI, thus requiring reliable high data rate with bounded latency. Third, **Physical awareness** totally relies on network sensing capabilities and positioning capabilities. One application example would be in an urban deployment to support traffic control at intersections. Finally, **Digital twins** may be of interest in large indoor industrial areas with blocking infrastructure thus requiring denser pico/femto cell deployments. There, network sensing and positioning is a must to create an accurate replica of the complex real-time environment.

Funded by the European Union

It is worth mentioning that we spotted another relevant use case for Industry 4.0 at the 3GPP-stage 1 workshop, presented by 5G-ACIA: **Time Sensitive Networks** (5G-ACIA, 2023)**.** This requires very accurate universal time synchronization between network nodes besides low latencies. It seems that over-the-air synchronization in 6G-REFERENCE can be an enabler for distributed cell free MIMO, but we also consider synchronization as a final application, providing accurate universal time.

3.1.1. Targeted KPIs

So far, we reviewed the functional and technical requirements for the proposed use cases in a qualitative manner. Table 1 compares the numerical KPIs provided by the ITU-R and the Hexa-X II project. Note however that ITU-R KPIs are provided in general, not targeting any specific use case, whereas the Hexa-X II project provides them per reference use case.

KPI	ITU-R	HexaX-II: Immersive experience	HexaX-II: Collabora-tive robots	HexaX-II: Physical awareness	HexaX-II: Digital twins
Peak data rate	50-100-200 Gbps	-	-	-	-
User experienced data rate	300-500 Mbps	250 Mbps	10 Mbps	1-10 Mbps 100Mbps (for sensor fusion)	100Mbps
Spectrum efficiency	1.5 to 3 times greater than IMT-2020	-	-	-	-
Area Traffic capacity	30-50 Mbps/m^2	20Mbps/m^2	-	-	-
Connection density	10^6-10^8 devices/km^2	-	0.1 devices/m^2	10^4 devices/km^2	1-10 devices/m^2
Mobility	50-1000 km/h	Seamless HO	20 km/h	300 km/h Seamless HO	100km/h

Latency	0.1-1 ms	10 ms (split rendering) 150 ms (collaboration)	0.8ms		1ms
Reliability	10^{-5}-10^{-7}	99.9-99.999	99.999-99.99999	99.99	99.99999
Positioning	1-10cm	10 cm	0.1-1m	1m	10 cm
Sensing	Yes	Yes	Yes	Yes	Yes

Table 1. Comparison of targeted KPI in (ITU, 2023) and (Hexa-X-II, 2023).

3.2. 6G-reference baseline deployment scenarios

The 6G usage scenarios addressed by 6G-REFERENCE, according to the diagram proposed by ITU-R, are shown in Figure 4.

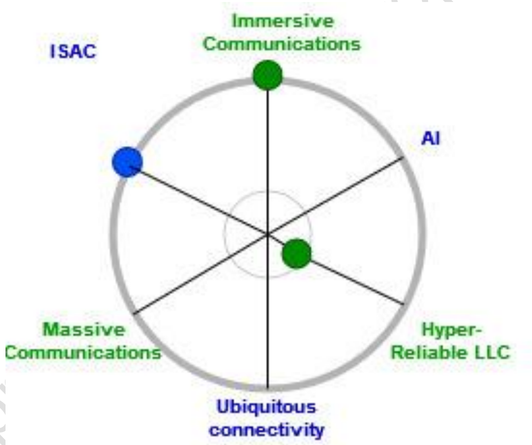

Figure 4. 6G-REFERENCE usage scenarios.

As introduced in Section 2, the goal of 6G-REFERENCE is to enhance user data rates and area capacity while providing awareness and environmental sensing information enabling new sensing-based services. Therefore, it mainly targets Immersive communications and ISAC. Accurate synchronization among the distributed nodes of the cell free deployment is crucial to enable coherent operation providing improved beamforming resolution and increased area capacity. However, 6G-REFERENCE also targets accurate over-the-air universal time synchronisation as a service itself. As identified in Section 3.1, this synchronization capability has a straightforward application

Funded by the European Union

to Time Sensitive Networks, which in 5G fell in the realm of URLLC. Although 6G-REFERENCE does not address enhanced reliability and latency, a small contribution to Hyper reliable LLC is included in Figure 4 to make explicit the goal of providing accurate universal time synchronization.

As a “hardware development” project, 6G-REFERENCE does not try to fulfil the specific requirements of any given use case. Instead, it develops technological solutions that should fit multiple use cases and applications falling within the usage scenarios identified in Figure 4. Therefore, next subsections identify three deployment scenarios, each of them tailored to address one of these usage scenarios, which in turn are directly linked with the first three system level challenges derived in Section 2: a communications-oriented scenario, a sensing-oriented scenario and a synchronization-oriented scenario. Note however that we only differentiate the main focus of the deployment, but each of them will address integrated sensing and communications and over-the-air synchronization mechanisms. The reason for the differentiation is to evaluate the full communication/sensing/synchronization capabilities of the developed technology without hard constraints coming from the other two capabilities. The last two system level challenges in Section 2, namely, the frequency selectivity and the requirement of low cost and low energy consumption are less clearly linked to the three deployment scenarios. Enhanced frequency selectivity may be required especially in outdoor deployments, but as we target cost-saving re-use of a single reference hardware design for a distributed RU in multiple scenarios, these will be considered general requirements.

3.2.1. Communications-oriented scenario: Urban square

This scenario focuses on providing enhanced user data rates and area capacity. Accurate time/frequency synchronization is considered as an enabler for distributed cell free coherent operation. Sensing and localization may assist communications (e.g. user-distributed RU association), realize immersive communication or become a service itself, but without significantly impacting communication performance. Figure 5 depicts the associated 6G usage scenario diagram, according the ITU-R classification.

Funded by the European Union

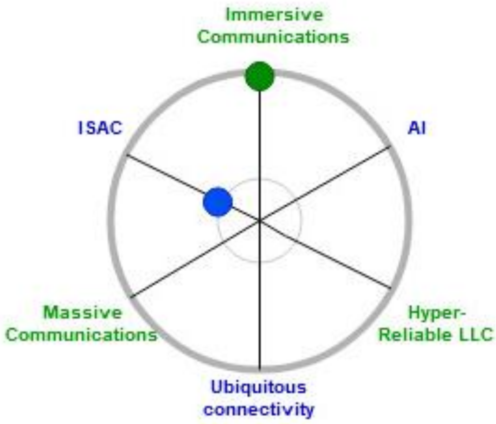

Figure 5. Urban square usage scenario diagram.

Scenario description: Open wide urban area, like an urban square, with a high density of users. It may include pedestrian areas but also some vehicle pathways and intersections. Although open, line-of-sight blockages are expected from large urban furniture or the presence of kiosks, trucks, etc. Users include, pedestrian, people in personal mobility vehicles or in slow cars and trucks. The area is covered with a rather dense distribution of RUs directly connected to a centralized processing unit or indirectly through another RU. In case of a direct connection, a mixture of cabled and over-the-air solutions can be considered. The dense deployment of RUs increases the probability of line-of-sight and reduces the distance between the users and the serving RUs. In some cases, Reconfigurable Intelligent Surfaces (RIS) can be deployed at some building walls to further improve the communication channel. Moreover, RIS can be exploited to extend the coverage beyond the urban square to the surrounding streets, by increasing the gain and angular resolution of single RU transmissions.

Supported use cases: The main use case here is the provision of high data rate links to all users to satisfy their requirements coming from any kind of new multimedia application. These may include immersive applications like XR, remote telepresence, holographic communication services, etc. In these cases, localization and integrated sensing will provide the connection between the real and digital worlds to realize the immersive experience. They can be also used to assist communications, for instance assisting the beam management or the association between users and RUs based on localization or permitting switching on and off some RUs according to the sensed user presence and density. Pure sensing-based use cases like traffic management at a road intersection, detecting and controlling pedestrian presence and mobility and gathering data of environmental sensors for e.g. air quality monitoring are also considered.

3.2.2. Sensing oriented scenario: factory/warehouse

This scenario focuses on providing accurate sensing and localization integrated with communications. However, required user data rates and area capacity are far lower than those in Urban square scenario, so more resources can be devoted to provide accurate sensing. As in the previous scenario, synchronization is considered here as an enabler for distributed cell free coherent operation. Figure 6 depicts the associated 6G usage scenario diagram, according the ITU-R classification.

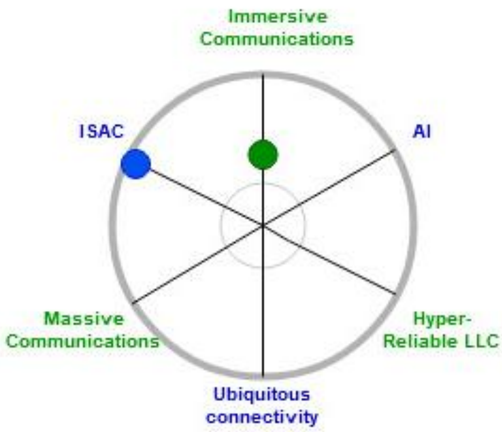

Figure 6. Factory/warehouse usage scenario diagram.

Scenario description: Large indoor complex facilities including large cranes, machines, robots, automatic guided vehicles, workers on motorized pallet trucks or similar and/or pedestrian workers. The area is largely obstructed by the presence of such large industrial furniture, so again dense RU deployment assisted by some RIS is considered to keep good propagation conditions. Again, the RUs are also directly or indirectly connected to a centralized processing unit, and a mixture of cabled and OTA links is envisaged.

Supported use cases: 6G-REFERENCE system provides communication services to workers and “intelligent industrial agents” (i.e. automated cranes, machines, robots, vehicles), requiring moderate to low data rate and area capacities. On top of that, it provides fundamental accurate sensing services. First, such a complex scenario mixing automated machines and human workers requires security measures to avoid collisions between machines/vehicles or accidents with workers. Therefore, sensing and localization services here include detecting and tracking workers and mobile agents and

Funded by
the European Union

predicting/avoiding collisions. Beyond this crucial application, sensing and localization can be also used to monitor and control pathways and intersections shared by automated and human-driven vehicles and to assist the operation of robots with a high level of autonomy. This use case can be extended to the full control of collaborative robots, but it would require reliability and latency requirements that are out of the scope of this project.

3.2.3. Synchronization-oriented scenario: Time Sensitive Networks

This scenario puts accurate time/frequency/phase OTA synchronization at the focus of the study. Although synchronization is a requirement to enable distributed coherent communications, here we delve a step deeper, considering universal time synchronization as an ultimate goal, as required in Time Sensitive Networks (TSN). Figure 7 depicts the associated 6G usage scenario diagram, according to the ITU-R classification. The contribution to the Hyper-Reliable LLC correspond to the provision of universal time synchronization as discussed previously.

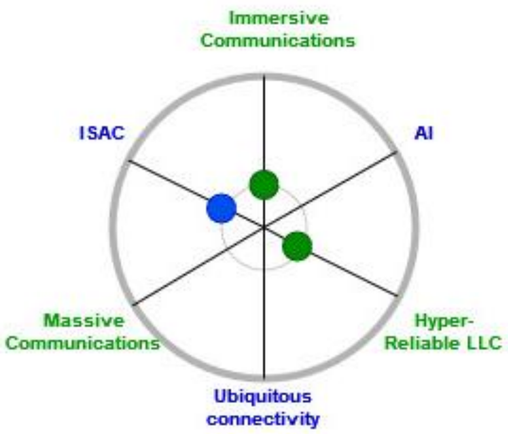

Figure 7. TSN usage scenario diagram.

Scenario description: The scenarios considered here can be the same in the previous two cases, that is open urban and large indoor industrial deployments. However, to stress out the synchronization performance, we reduce to the minimum cable connections, so most of the RUs are connected through OTA links. Moreover, the number of cascaded RUs requiring multiple hops to reach the centralized processing unit, which is the one providing the network synchronization reference, is increased. This, in general, corresponds to simplified less-invasive deployments, requiring less anticipated planning and thus resulting in more flexible solutions. In addition, here we favor indoor deployments since they cannot rely on GNSS solutions for providing universal time synchronization. Note however, that outdoor deployments are not fully discarded, since there is a generic interest in developing self-contained 6G networks not depending on external services like GNSS.

Supported use cases: The baseline use case here is the provision of time/frequency/phase synchronization required for coherent distributed communications, even in the case of OTA multi-hop connected RUs. However, the ultimate application is the provision of universal time synchronization, required in TSN, which typically correspond to industrial deployments requiring time synchronization among different automated agents like robots, machines, cranes, etc. However, as identified by ITU-R (ITU, 2023), some Immersive communication would also require time synchronized transmissions becoming kind of TSN applications. Let us remark that the industrial application of TSN requires also high reliability and low latency, which are out of the scope of the 6G-REFRENCE goals.

3.3. Baseline system architecture

This section provides a high-level overview of a 6G system based on 6G-REFERENCE ideas in order to show how they fit in the overall system level architecture. Currently, there is no agreed baseline architecture for 6G networks. However, it could be envisaged that for high population density areas, the resulting architecture will combine and extend the cell-free and cloud-RAN concepts. This translates to a high densification of distributed RUs on a cloud-RAN fashion, which decouples hardware and software functions, virtualizing RAN operations. Such virtual functions are then split between centralized processing units (CU), distributed processing units (DU) and the distributed RU themselves. Note here that the current 5G terminology is used to describe potential 6G network elements, leveraging on a likely evolution from 5G rather than on a disruption, as claimed by multiple industrial associations.

Figure 8 depicts a generic system level view for this architecture. It consists of multiple distributed RUs connected directly or indirectly to a single or multiple centralized processing units, namely DU/CU+DU. 6G-REFERENCE does not care about how the RAN functionalities are split between CU and DU, it focuses on how they are split between CU+DU and RU, with special focus on how distributed beamforming is handled.

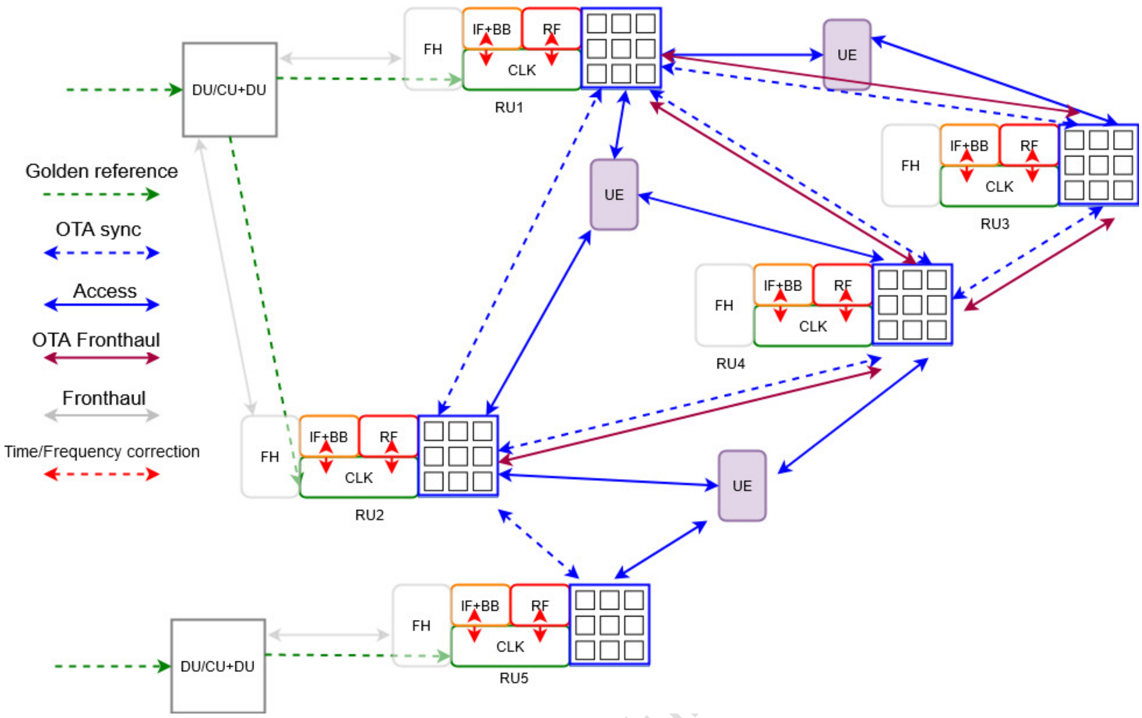

Figure 8. System level Architecture.

In order to address the design of the RU in a generic way that could fit multiple specific deployments, as the ones discussed in previous sections, three different cases are exemplified. RUs 1 and 2 are directly connected through the fronthaul to the same CU. This connection not only transports data but also distributes the master frequency and timing reference to all RUs, denoted here as the "golden reference." We assume here that in massive cell-free deployments, this fronthaul and synchronization link will not always rely on fibre, but also on wireless solutions, which will not only provide more noisy references, but also provide them in a discontinuous form with larger holdover periods. Improvements in OTA synchronization between the different RUs will be developed to provide better synchronization accuracy and address time/frequency misalignments introduced by the fronthaul link and the RU hardware. The second case is exemplified by RU3 and RU4 that do not have a direct connection to the CU. Instead, they are in fact cascaded to RU1 and or RU2. In this case, OTA synchronization is crucial to enable coherent transmissions from the distributed RUs. Moreover, beam scheduling flexibility and increased capacity are required for an efficient fronthaul data distribution involving these RUs. The third case corresponds to RU2 and RU5, that are ideally coherently transmitting to the same UE but are attached to a different CU, which may happen often in a densified cell-free deployment. In this case, direct OTA synchronization between RUs likely improves timing and frequency synchronization across multiple RUs. In all these cases, the aim of synchronization mechanisms is to provide time alignment at the RU's array planes. The potential time difference of arrival to the different users can for communication be tackled by L1 processing mechanisms, but better time-synchronization at array panel level can relax L1 requirements and hence substantially reduce the time and frequency resources otherwise allocated for such processing. Note moreover, that coherent transmission for radar sensing cannot rely on L1 processing, which increases the time alignment requirements at the RU array planes.

The distributed architecture discussed above makes evident two of the main 6G-REFERENCE challenges: the need for accurate OTA synchronization and for an efficient data distribution at fronthaul level. The next subsection describes the enablers to be included in each distributed RU to accomplish not only these challenges but also the joint communications and sensing from the same hardware and the increased frequency selectivity with practical radios with associated low cost and low power consumptions.

3.4. Baseline Radio Unit architecture

The main enablers for the 6G-REFERENCE solution can be listed as follows, where 1-3 address communication challenges, 4-5 synchronization challenges, 6-8 integrated sensing and localization challenges and 9 frequency selectivity challenge.

1. Increased capacity on fronthaul links by full-duplex (FD) transmission/reception
2. Efficient concurrent multi-beam operation through Time Modulated Arrays (TMA)
3. Extended beamforming performance of single arrays through RIS-based solutions
4. Low Phase Noise frequency generation with OTA frequency synchronization
5. Full-duplex high update-rate timing synchronization (FDsync) between RUs, providing high resolution universal time synchronization
6. Increased self-interference cancellation (SIC) to support monostatic radar
7. Localization with high resolution through Frequency Modulated Arrays (FMA)
8. Integrated environmental sensors
9. Frequency selectivity to reject adjacent in-band and out-of-band interferers

Figure 9 sketches the architecture of the envisioned RU including all hardware enablers.

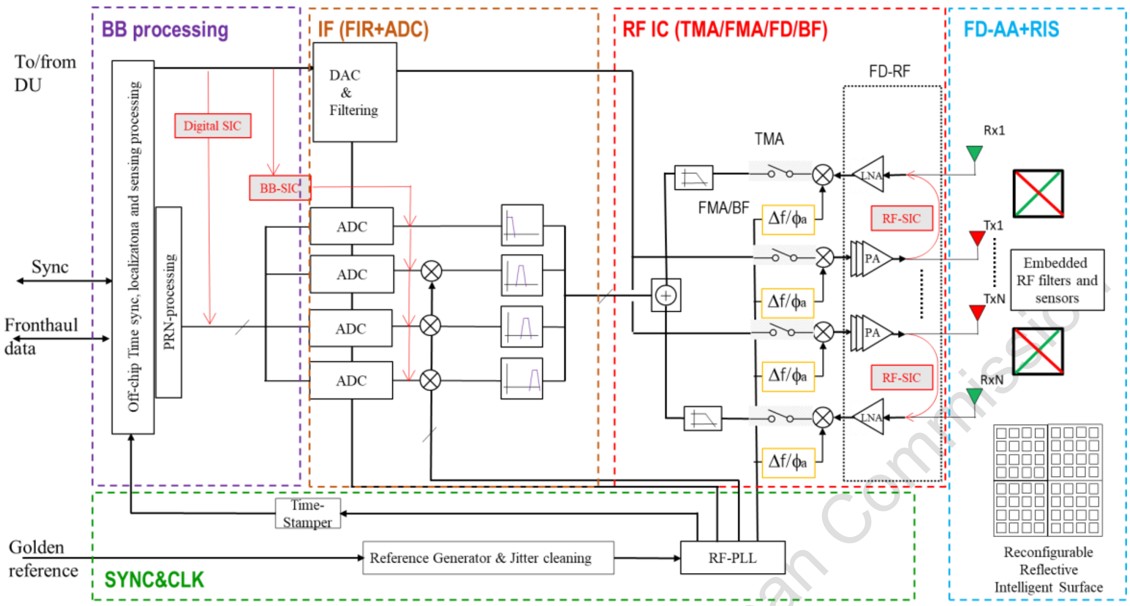

Figure 9. RU architecture.

From right to left, we start by antenna solutions including an antenna in-package design providing low coupling between Tx and Rx elements for FD operation and integrated RF filtering for frequency selectivity (FD-AA), and a reconfigurable RIS to expand the capabilities of small arrays at an affordable cost while integrating environmental sensors (RIS). At radiofrequency stage (RF) the RU uses phased array technology with SIC for FD operation (RFIC-FD), and complementary/alternatively TMA and FMA efficient solutions for concurrent multibeam data distribution and localization, respectively (TMA/FMA). The IF stage includes highly programmable FIR-filtering to support different IF-frequencies and channel bandwidths and support the TMA operation that maps different beams to different IF-frequencies (FIR-IF). Moreover, A/D conversion (IF-ADC) is provided at low enough frequencies to be power efficient, and down-conversion mixing in case of non-zero IF channels. For the baseband (BB) and digital domain, the RU includes BB SIC solutions reinjecting signal before the ADCs. Correlators are implemented in the digital domain for the detection and alignment to Pseudo Random Sequences for synchronization and sensing (XC-PRS), and monostatic radar processing. Finally, the RU includes frequency generation circuits with jitter cleaning for Over the Air Synchronisation exploiting new high-frequency Crystals (RFXO-PLL and RF-SYN). In addition, an RF digital PLL with hardware time-stamping capabilities will enable accurate frequency and phase synchronization, while also supporting high-resolution PTP time-stamping to UTC.

4. System Specification

4.1. Deployment Scenario

The deployment scenario, considered in this project, focuses on achieving uniform coverage with a distributed MIMO network in a 100m x 100m area of an outdoor urban square and indoor industry warehouse. The urban square use-case would require the network and the RUs/APs to handle communication-centric requirements related to capacity and latency. The industrial use-case would instead focus on sensing performance with communication related metrics still being relevant. In both use-cases support for Time Sensitive Networking will also be considered.

Figure 10 illustrates two options for regular deployment grids with a single DU for an indoor scenario. While the deployment in an urban square could have a more irregular grid, the maximum inter-RU distance is assumed fixed to 25 meters in link calculations. The targeted performance metrics for communication in an outdoor urban area are listed in Table 2. While the user experienced data rate and latency are as per ITU-R KPI (listed in Table 1), targeted connection density and peak data rate in Table 2, corresponds to the number of devices considered reasonable for urban square scenario. Since the cascaded deployment topology in Figure 10 needs to support data forwarding across RUs within the latency limit, fronthaul segments with varying capacities could be used for different parts of the grid.

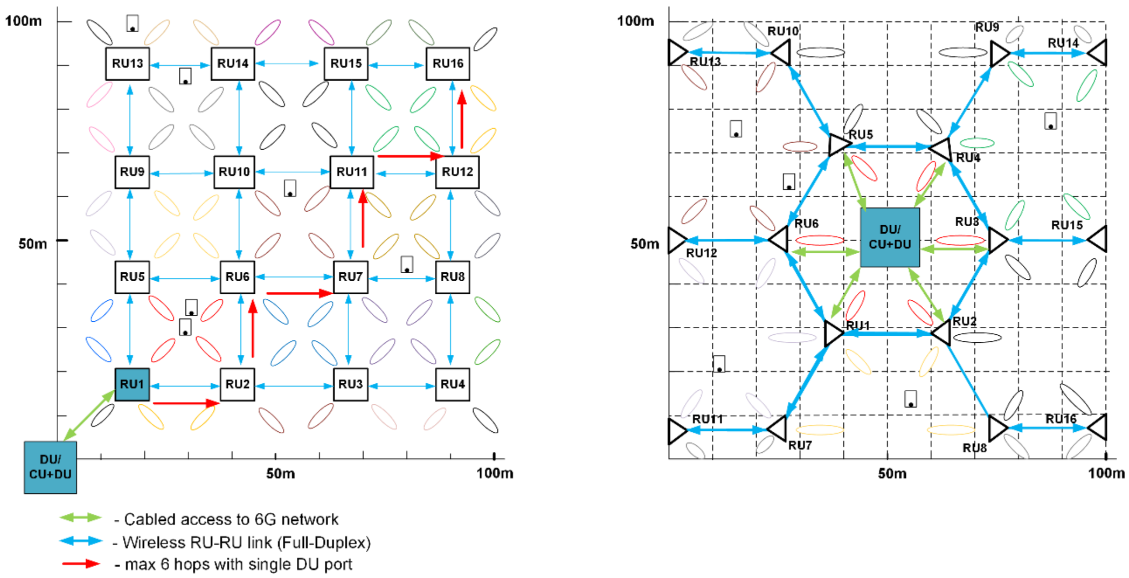

Figure 10. Illustration of a regular D-MIMO grid for indoor deployment.

Each RU is assumed to have (at least) 3 antenna array panels to support data forwarding and reception in all directions. As a general case, RUs with an array size of 16 elements are assumed for the following link calculations. Full-duplex communication with a higher modulation scheme (256-QAM) and wide bandwidth (400MHz), is targeted in this project, for enhancing data throughput in point-to-point wireless links between RUs. To keep fronthaul segment capacity greater than the access capacity, each RU panel is assumed to co-schedule at maximum 4 UEs per slot with full bandwidth and relatively lower modulation scheme (64QAM, 4 times lower than 256QAM). Each UE is assumed to be served by 1 to 4 RUs, with the access and fronthaul link using the same 14.8-15.35GHz band.

Urban square deployment		
Connection Density	10^5 devices/km^2	Assumed 1000 devices for 100mx100m space
User experienced data rate	480 Mbps	160MHz (20% Guard band) x 6 bits (64-QAM) x 0.5 (Bit rate efficiency)
Peak data rate (AP-UE Link)	23 Gbps	320MHz (10%-20% Guard band) x4 beams x6 bits (64-QAM) x 2 polarizations x 0.5 (Bit rate efficiency)) x 3 panels
Area traffic capacity	43 Mbit/s/m^2	$\frac{\text{Peak data rate}}{\pi.(13)^2}$ for each RU covering a radius of 13meters
Latency	0.1-1 ms	6 hops (or) radio slots as delay (wherein 1 slot = 125μs for SCS = 120kHz)

Table 2. Performance objectives for communication in urban square D-MIMO deployment.

Sensing requirements for the use-cases of urban square and industry warehouse, listed in Table 3 and Table 4 are referred from 3GPP-22.837 (3GPP, 2024c).

Outdoor urban square	Range Resolution	Velocity Resolution	Latency [ms]	Missed Detection [%]	False Alarm [%]	Confidence Level [%]	Refreshing Rate [s]
Human	1m	1m/s	1000	2-5	5	95	0.2
Vehicle	1m	1m/s	100 - 1000	2	2	95	0.05-1
UAV	1m (Tracking) 10m (Detection)	1m/s (Tracking) 10m/s (Detection)	100 - 1000	2	2	95	0.05-1

Table 3. Sensing requirements for urban square deployment.

Indoor Industry Warehouse	Range Resolution	Velocity Resolution	Latency [ms]	Missed Detection [%]	False Alarm [%]	Confidence Level [%]	Refreshing Rate [s]
Human	0.5m	0.5m/s	100 - 5000	1	3	99	0.1
AGV/AMR	0.5m	0.5m/s	100	-	-	99	0.1

Table 4. Sensing requirements for industrial warehouse deployment.

4.2. Communication specification

In a D-MIMO network, while each single RU should support the capacity required for fronthaul relaying, the multi-RUs serving the UE should support co-ordinated interference management in a dense user scenario. RUs with an array size of 16 elements are considered as an initial assumption satisfying the required fronthaul capacity for serving co-scheduled UEs, while aiding the diversity with array gain in the access link.

The following section focuses on the link budget for fronthaul and access that is achieved with a single RU frontend, assuming enough resource block are allocated to the fronthaul link keeping its capacity greater than the access link. The Waveform and Numerology assumed are aligned with 5G-NR.

Funded by the European Union

4.2.1. Inter-RU Link

The RU specification, listed in Table 5, highlights the use of a higher modulation scheme and bandwidth in full-duplex mode to handle the capacity needed for fronthaul load. In addition, the sub-carrier spacing (SCS) of 120kHz with its slot duration of 125μs, could allow maximum 6 hops over the aggregating RUs, for attaining the desired latency of less than 1ms.

The useable bandwidth is calculated with an assumption of 20% being allocated to guardband. Based on the refinement of coexistence specification (Section 4.5), the guardband allocation would be limited at the further stage of the project. The link margin with a conservative value for handling blocking scenarios, would be also revised in the following stages of the project, towards implementing low-power RUs for distributed MIMO network.

RU Parameters		
Frequency	14.8GHz-15.35GHz	
Bandwidth	400MHz	
SCS	120kHz	
Path Loss	84dB@25m	
Modulation	256 QAM	
EVM_{Tx}	3.5%	
NF	7dB	
SNR_{Rx}	30dB	
$EIRP_{Tx}$	30dBm	*Average power for 256 QAM transmission*
$Sensitivity_{Rx}$	-60dBm	*-174dBm/Hz+10log(BW)+ NF + SNR -10log(16)+ IL(4dB)*
$P_{Rx,max}$	-53dBm	*$EIRP_{Tx}$ - PL*
Link Margin	19dB	*$EIRP_{Tx}$ - PL +10log(16) - $Sensitivity_{Rx}$*

Table 5. RU specification for data forwarding via a fronthaul link.

4.2.2. Access Link

While the fronthaul link has a static LoS channel, the access link to UEs is a dynamic channel environment. Ideally, coordinated multi-RU fully coherent transmission brings 6dB extra received UE-power per doubling of the number of coordinated transmitters, but practical gains will be limited by coherency errors and blockers. Interference-suppression precoding may allow for improvements in SINR, and thus throughput. Figure 11 (Lin and Haliloglu, 2022) reports an increase in downlink spectral efficiency, achieved through spatial multiplexing gain with coherent transmission from 4 RUs, in a pessimistic use-case scenario with 1000 blockers. The scenario in Figure 11(a) models UE mobility up to 5m/s and distributed blockages of size up to 2mx3m. Figure11(b) also highlights the non-coherent transmission performance being worse due to the lack of optimized parameters for interference cancellation. For non-coherent transmission, the UE needs to implement successive interference cancellation to decode the individual streams which renders a penalty on data rate and complexity (Ammar, Adve, Shahbazpanahi, Boudreau, & Srinivas, 2022). The project thus focuses on phase alignment/ synchronization between RUs as one of the major hardware enablers for spectral efficiency improvement with coherent transmission.

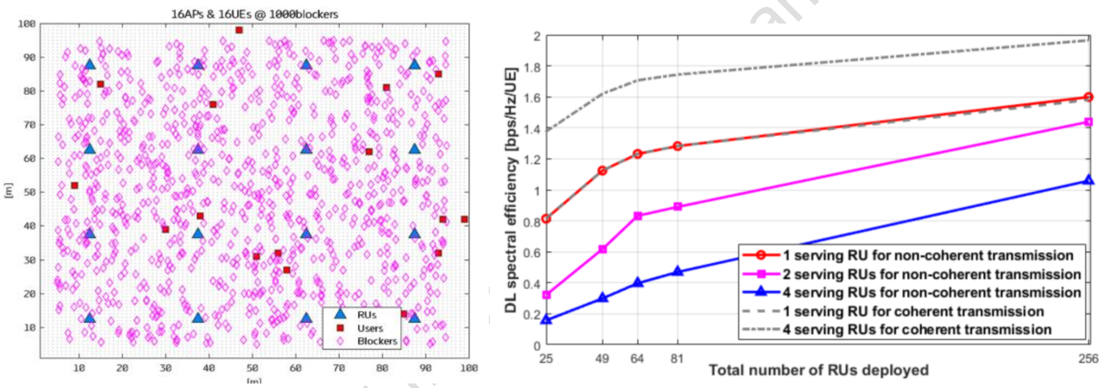

(a) (b)

Figure 11. (a) Illustrative deployment scenario with 16 UEs and 1000 blockers (b) Spectral efficiency performance for different number of serving UEs (Lin and Haliloglu, 2022).

Table 6 indicates the link budget with the same RU frontend being used for access, as for fronthaul. The coherent transmission from multiple RUs is added similarly as array gain in the link calculation, theoretically indicating an SNR improvement to that achieved with co-located antenna arrays.

RU Parameters for Downlink		
Frequency	14.8GHz-15.35GHz	
Bandwidth	50MHz, 100MHz, 200MHz,400MHz	
SCS	60KHz, 120KHz	
$EIRP_{RU,Tx}$	30dBm	

Path Loss	84dB@25m	
Modulation	64-QAM	
$EVM_{RU,Tx}$	6%	*EVM_{Link} = 10%*
NF_{UE}	7dB	
$EIS_{UE,Rx}$	-64dBm *(400MHz)* -73dBm *(50MHz)*	*9dB sensitivity variation based on BW.* *-174dBm/Hz + 10log(BW) + NF + SNR -6dB (Antenna gain) + IL (4dB)*
Link $Margin_{DL}$	10dB *(400MHz)* 19dB *(50MHz)*	*$EIRP_{Tx}$ - PL - $Sensitivity_{Rx}$*

RU Parameters for Uplink		
Received power ($P_{RU,in}$)	-72dBm	$EIRP_{UE,Tx}$ (12dBm) – PL(84dB@25m)
$NF_{RU,Rx}$	7dB	
$Sensitivity_{RU,Rx}$	-69dBm *(400MHz)* -78dBm *(50MHz)*	-174dBm/Hz+10log(BW) +NF+SNR (25dB)-10log(16)
Link $Margin_{UL}$	9dB *(400MHz)* 18dB *(50MHz)*	$EIRP_{UE,Tx}$ -PL+10log(16)-$Sensitivity_{RU,Rx}$

	Single-RU	Multi-RU
SNR_{Link}	20dB	32dB *(4-RUs)* (Theoretical upper-bound with perfect phase alignment. channel state information and fronthaul network)

Table 6. RU specification for access link to UE.

4.3. Sensing specification

Sensing functionality is targeted in the defined network for industrial/urban use case with reuse of the same spectrum (14.8GHz-15.35GHz) and RU resources as communication functionality. The desired sensing performance metrics for the application scenario are summarized in Table 7. Based on the probability of detection and probability of false alarm (specified in Table 3 and Table 4) in receiver operating characteristics (ROC) curves., the SINR of 15dB is targeted for sensing

Sensing specification	
Range (R_u)	25m

Range resolution (R_r)	0.5m
Spatial/Angular resolution	6°
Velocity Resolution (v_r)	0.5m/s
Unambiguous Velocity (v_u)	6m/s *(Slow Vehicular AMR)*
Signal Bandwidth	400MHz
SINR *(after range processing)*	15dB

Table 7. Sensing specification for the use-case scenario

The range resolution, defined as the minimum distance to distinguish two different targets is dictated by the following formula:

$$R_r = \frac{c}{2\,BW}$$

Hence a minimum 300 MHz bandwidth is required to achieve 0.5m resolution, which is feasible.

The timing parameters relevant to sensing waveform are derived in Table 8, from the sensing specifications. The requirement on unambiguous range (R_u) and unambiguous velocity (v_u) places the minimum and maximum bound {$T_{r,min}$, $T_{r,max}$} on repetition rate of sensing symbols. The velocity resolution specification places requirement on the minimum sensing frame duration ($T_{f,min}$) , as per the following formula:

$$v_r = \frac{\lambda}{2.M.T_r}$$

Considering $\boldsymbol{\lambda}$ =0.02 m, the required velocity resolution of 0.5m/s could be achieved with M=24 sensing symbols repeating with periodicity of $T_{r,max}$ = 0.83ms in a single frame.

While the sensing waveform could be optimized separately than communication, the sensing signal is expected to be compatible with OFDM symbol duration (e.g. 8.3μs symbol duration for 120kHz subcarrier spacing).

Sensing Signal Parameters @15GHz	
Maximum time interval between sensing symbols	$T_{r,max} = \frac{c}{4v_u f_c} = 0.83ms$
Minimum time interval between sensing symbols	$T_{r,min} = \frac{2R_u}{c} = 172ns$
Minimum sensing frame/burst duration	$T_{f,min} = \frac{c}{2v_r f_c} = 20ms$

Minimum Bandwidth	$BW_{reqd.} = \frac{c}{2R_r} = 300MHz$
Ratio of sensing to communication signal in time	20%
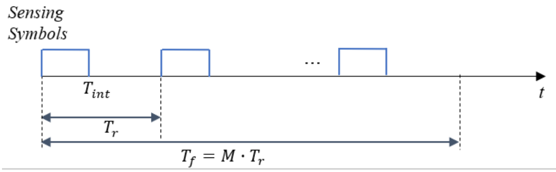	

Table 8. Sensing signal timing based on the specification.

4.3.1. Communication-centric Design Choices

Considering that this project largely has a communication-centric rationale, hardware design focusses in the first place on communication requirements. The idea is to save costs and add functionality by re-using the communication hardware preferably with minimum adaptations for radar. In principle a communication OFDM-waveform can be used as radar signal, but there are certainly trade-offs, e.g. compromises in performance for range and Doppler speed estimation. This is noticeable when studying the radar ambiguity function and the related range and Doppler target profiles. To improve performance we allow for up to 20% time-budget for radar and localization, which may further operate with a low duty cycle depending on the application scenarios. We aim to explore adapted waveforms while re-using the communication hardware, amongst which an OFDM waveform with reduced PAPR (Bourdoux, 2024). Algorithms will be developed to mainly estimate the range, velocity and AoA of the radar targets.

4.3.2. Geometrical Specification of the Radar scenario

For radar simulations it is important to describe the geometry of the radar scenario in a bit more detail (see Figure 12) and define simulations to characterize the range, velocity and AoA detection capabilities. Frequency analysis based on Doppler effects allow for estimating the velocity of the target and providing AoA information. The processing can be summarized in two main steps: one devoted to the temporal processing, i.e. to the ranging of the target, the second, namely the spatial processing, aimed at identifying the direction and kinematics of the target motion. The maximum range of detection is related to SNR, calculable through the radar equation, and to the interpulse lapse, or Pulse Repetition Frequency (PRF). Minimum detectable Doppler velocity fixes the velocity resolution. Figure 12(a) and Figure 12(b) show the main parameters used by Radar processing to sense the targets and an example of the geometry of the deployment scenario (Indoor Industry Warehouse case) respectively. In this case we refer to a monostatic acquisition mode; a bi-static mode could be also evaluated based on the use of the Tx of an AP and the Rx of a different AP. This configuration could improve the detection of target with particular scattering pattern but demands an accurate time synchronization between the different units.

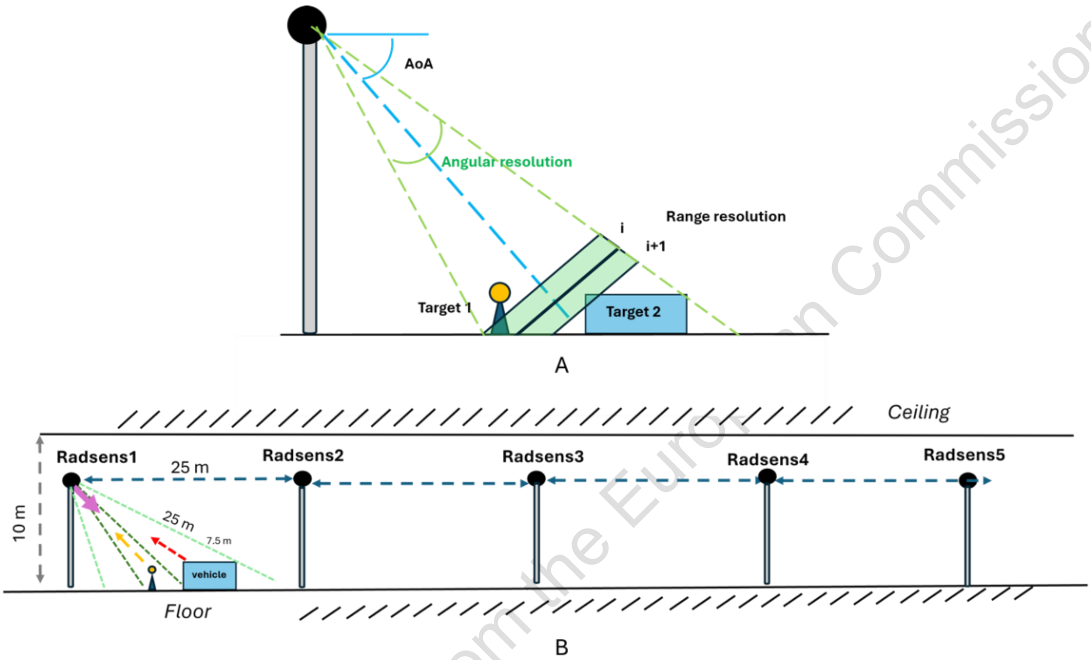

Figure 12. a) Parameters used to detect targets according to the Radar processing. b) Illustration describing the geometry of the deployment scenario (Indoor Industry Warehouse case).

4.4. Timing and Synchronization specifications

Cell-free, rapidly deployable radio units require synchronization to be over-the-air (OAS). This means that these radio units do not have access to the wired "golden reference" timing information, but instead must synchronize wirelessly. In the project proposal we mentioned the following initial target requirements:

- UTC Time resolution <100ns
- Frequency inaccuracy <0.01ppm
- Jitter < 100fs

During the system level study, we have confirmed that these requirements make sense for communication and Time Sensitive Networks, but also found that some sensing scenarios (e.g. bi-static radar) may require an even better frequency accuracy of 1.6ppb to keep the carrier frequency drift between transmitter and receiver lower than the velocity resolution for Doppler speed detection (see sensing specification in Section 4.3).

Moreover, we have studied D-MIMO requirements in more detail. To enable coherent downlink transmission to UEs in D-MIMO, phase synchronization between the transmitters and receiver is required (Madhow *et al.*, 2014). For two aligned phase coherent transmitter this ideally doubles the received amplitude. If we (somewhat arbitrarily) assume that 0.7dB loss due to phase misalignment is allowed, the phase offset between the signals received by the receiver must be less than approximately 45 degrees (±22.5 degree per RU). This translates to a maximum absolute time offset of approximately ±4ps at a carrier frequency of 15GHz. For realizing interference nulling in the order of 10dB-20dB, calculations show that tighter phase alignment, in the range of 30° to 10°, is required among RUs. This is a very challenging requirement, especially as we need to achieve this via a wireless link. Further research is needed to find out what is feasible in practice, and this is one of the key research questions for the timing part.

During uplink, the time alignment between RUs could be relaxed to a fraction of the cyclic prefix (CP= 0.59us for SCS=120kHz) (Ruffini *et al.*, 2021) as the DU conducts coherent combining of the data streams to multiple RUs with equalization based on channel estimation. We conclude that tighter synchronization is required between the RUs during the downlink access compared to the uplink.

Table 9 summarizes the discussed requirements on inter-RU synchronization, with respect to coherent transmission and sensing application. In case of monostatic sensing, static time and phase alignment errors between transmit/receive synthesizers could be removed in range-profile post processing. However, synthesizer's phase noise has an impact on range sidelobe level, and the requirement for the same would be derived in further course of the project, based on the choice of sensing waveform.

RU Parameters	Value	System Requirement
Frequency Stability	1.6ppb	*Doppler speed for stationary target due to carrier frequency drift from Tx to Rx, kept less than the velocity resolution;* $v = \frac{\Delta f}{f} * c$
Phase Alignment Error	<45° *(for coherent combining in downlink, ±22.5° per RU)* <30° *(=10dB interference nulling)* <10° *(=20dB interference nulling)*	

Time Alignment Error	100ns	*For Uplink , tolerable time alignment error is fraction of cyclic prefix*

Table 9. Synchronization specification for coherent transmission and sensing requirement

Finally, we studied requirements on time-stamping traceable to UTC and looked at the state-of-the-art. Time-stamping to UTC requires a certain long term frequency stability. GNSS systems such as GPS offer microsecond range accuracy (Bogdanov *et al.*, 2018) but do not work indoor. PTP (IEEE1588) provides sub-microsecond accuracy in wired applications (Eidson, 2005), but suffers from degraded accuracy when transmitted using WiFi protocols (Mahmood *et al.*, 2017). This degradation is mainly related to large delay uncertainties in package transmission and software time stamping. These issues can be addressed by keeping delays in check and using hardware time stamping (Mahmood *et al.*, 2017). By doing so, e.g. exploiting low delays enabled by full duplex, we believe we can achieve time-resolutions below 100nsec, which is about 10x better than PTP and goes also roughly 10 times beyond what GNSS systems can offer. As it is also in line with what standardization organizations have mentioned as future target, we decided to stick to this 100ns target as goal specification.

4.5. Coexistence specification

Cellular operation using the cm-wave frequency range needs to co-exist with existing services. In this project we intend to use the frequency band 14.8-15.35 GHz allocated to cellular services. However, the neighbouring frequency band 15.35-15.40 GHz is used for Earth Exploration-Satellite Service (EESS) and there will therefore be stringent requirements on emissions for those two frequency bands with their respective operations to co-exist. As the cellular frequency band 14.8-15.35 GHz has not yet been standardized, there is currently no specification available and the work on this in 3GPP will most likely not happen until late 2025. In (3GPP, 2024b) in-band and out-band emission requirements are specified for FR1 and FR2 and can be used as guidance. Limits for protection of Earth Exploration Satellite Service have also been specified for the 23.6-24 GHz EESS frequency band in (3GPP, 2024b) and can be seen as indicative for the EESS bands around 15GHz.

A common method for two neighbouring frequency bands to co-exist is to introduce a guard band between them. This allows for filtering of emission products but at the same time the guard band is wasted frequency that cannot be used for any service and therefore the guard band should be as small as possible. A small guard band allows for better spectrum usage but requires high quality filters with a steep roll-off which tends to be costly and difficult to manufacture. Another option is to put tougher linearity constraints on the active circuits to lower the emissions. This on the other hand tends to increase the power consumption. During the 6G-REFERENCE project we will explore what is feasible and propose a specification and solution that combines filtering and improved linearity (ACLR) to fulfil the co-existence requirements with the neighbouring EESS frequency band.

5. Block-level specification

5.1. FD-AA, RIS-AA

This section contains the specifications regarding the antenna array and reconfigurable intelligent surface building blocks.

5.1.1. FD-AA

The target antenna for full duplex operation is a 16-element array with dual polarization. The projected access point will contain 3 antenna panels, each with an angular range of $\pm$60° in azimuth, while elevation range being decided based on deployment scenario.

Based on initial explorative antenna array simulations and Full Duplex link budget calculations, we propose to target an isolation between elements of over 30dB for the target 400MHz bandwidth. Higher isolations can likely be accomplished considering integrated decoupling structures or grounded elements. As antenna element coupling is significantly higher when using the same polarization for transmission and reception, orthogonal polarizations are desired. However, it is also possible to double communication capacity directly by using 2 polarizations, hence using polarisation isolation for full duplex antenna isolation is preferably avoided.

The antenna array will be designed to operate in the 14.8-15.35GHz band. The antenna elements of the FD-AA building block include integrated filtering function to suppress out of band emissions in the 15.35-15.40GHz frequency range. There is a significant trade-off between the guard bandwidth and the out-of-band rejection and antenna gain roll-off at the band edge. For example, considering a guard band of 80MHz, the projected antenna gain of the filtering antenna is in the range of 6.5dB with a roll-off of 3dB at the band edge, using planar antennas. Modular 3D filtering antennas with higher gain will be explored as alternative.

The level of rejection that can be provided by an integrated filtering antenna will be much dictated by the width of the guard-band as well as any requirement for gain flatness in the operation band. When designing an antenna with an integrated filter, we can choose between bandpass filters that eliminates a wide range of frequencies, or notch filters that target a specific frequency range. Implementation challenges include the need to use different filters for each polarization and ensuring that these filters are compact enough to be integrated within the antenna array.

Figure 13 illustrates a typical response of a filtering antenna. Like filters, filtering antennas can use transmission zeros (TZs) to reduce out-of-band emissions. Generally, the closer the TZ is to the operating band, the lower the suppression level. At least two upper TZs are required for effective attenuation of over 30dB near stopband considering a resonator unloaded quality factor of 800. Filtering unwanted radiation is a challenge associated with the filtering antenna design, shape and materials. Both planar and 3D structures are being considered for filtering antennas, with a trade-off among size, complexity and performance.

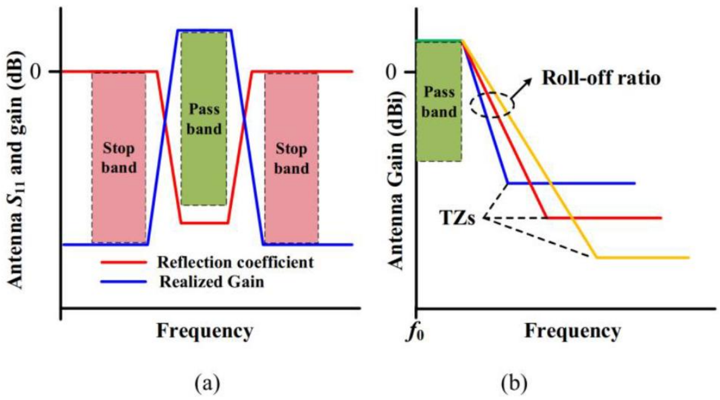

Figure 13. Filtering antenna typical response.

As an estimate, for the concerned passband of 6G-REFERENCE and a guard band of 80 MHz, it is feasible to achieve at least 10dB rejection from an integrated antenna within the same footprint of a conventional patch. Our initial design has achieved a 13 dB rejection. If the guard band can be relaxed to 100MHz, a 20dB rejection may be achievable over the no-emission band. More rejection may be achieved by either using external filters or by cascading more resonators to the filtering antenna. In both cases, however, there will be a trade-off in terms of antenna profile and the insertion loss.

5.1.2. RIS-AA

As discussed in Section 3.2.1, we propose to use reconfigurable intelligent surface (RIS) in 6G-REFERENCE in two ways. Firstly, we aim to use it as an intelligent reflector, to reconfigure antenna beams as shown in Figure 15(a). The RIS aperture is used as a focusing system providing larger gains and reduced beamwidths for communications and sensing. Indeed, the integrated array discussed in previous section 5.1.1. and the RIS form a reflectarray antenna where the integrated 16 element array in 5.1.1. acts as the feed. The RIS will provide coarse beam steering capabilities to illuminate a given sector whereas feed array beam steering provides fine tuning capabilities within that sector. As a result, the RIS can be used to extend the range, agility and improve the angular resolution of single RU transmissions, for instance for narrow streets connected to a main urban square in which a dense grid of RUs is already deployed, or to extend the coverage to long corridors or specific areas in large indoor factories or warehouses.

The required size of the RIS in this case depends on the required resulting gain and beamwidth, which are related to the communication range and spatial discrimination. Figure 14 compares the gain obtained with a square reflectarray antenna of side length L and a feed array of 4X4 elements. Preliminary simulations were performed modelling the feed array patterns with a $\cos^{28}(\theta)$, which approximates reasonably well the main beam of the feed array (Yngvesson, K.S. *et al.* 1988). It can be observed that for an operating frequency of 15GHz, a moderate RIS with L=21cm, which may include 441 elements at half-wavelength spacing, provides already a gain improvement around 12dB that can be translated to an extended communications range of 100m keeping the same link margin.

Funded by the European Union

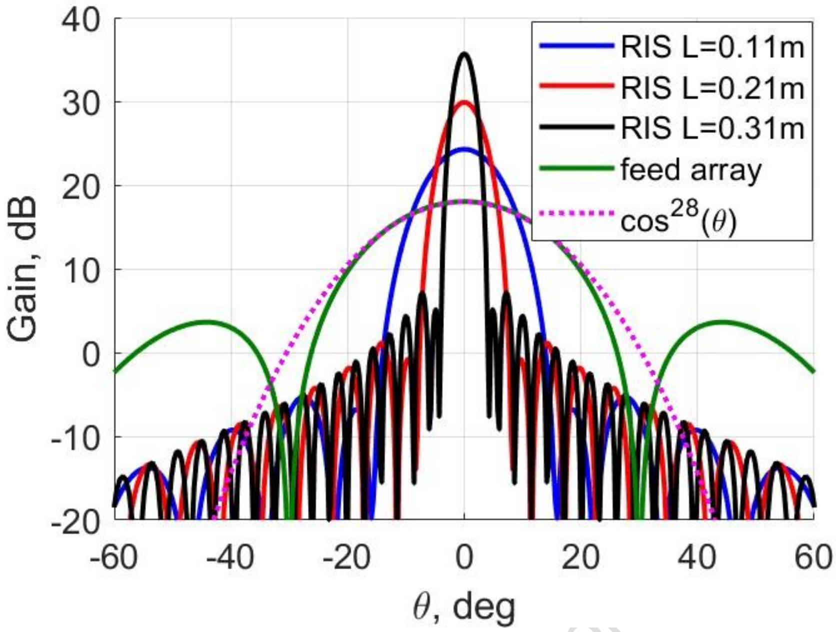

Figure 14. Radiation pattern comparison with a square RIS with a side length L and without RIS.

Secondly, the RIS can be used as an anomalous reflector (Vuyyuru S. K. R., *et al.* 2023) or mirror to provide reflected beam reconfiguration as shown in Figure 15(a), or avoid obstacles, e.g. in the factory environment, providing reconfigurable non-line-of-sight signal paths as shown in Figure 15. Reconfigurable intelligent surface use case scenarios, (a) RIS used as an intelligent reflector, (b) RIS used to reconfigure signal paths around obstacles (e.g. in a factory environment). Reference (Di Renzo *et al.* 2020) demonstrated that for this application the system behaviour depends on the size of the RIS versus the length of the communication path. A large RIS behaves as an anomalous reflector capable of redirecting the received signal to the direction of the intended user. A small RIS behaves like an intelligent diffuser. Frequency scaling the results obtained in (Di Renzo *et al.* 2020) to 15 GHz leads to the conclusion that a RIS with a side length of 93 cm would behave as an efficient mirror up to 186m. Therefore, for practical scenarios requiring shorter distances, much lower RIS sizes can be foreseen. Even the 21 cm RIS discussed in the reflectarray case of Fig. 15a would have an application to most intended scenarios.

In both cases, the projected RIS elements will support dual polarization and operate from 14.8 to 15.35 GHz, whereas the required size of the RIS will be defined together with the FD-AA building block described in section 5.1.1. It will include a control system that allows reconfiguring the reflection phase of individual RIS elements and will include shift registers to provide a logical switching sequence to antenna elements simultaneously, voltage regulators to bias solid state diode components and a microprocessor to operate beam reconfiguration of the RIS. The unit cell comprises one vertical element and one horizontal element to ensure dual polarization, and thus reflection phase reconfiguration of the reflected wave.

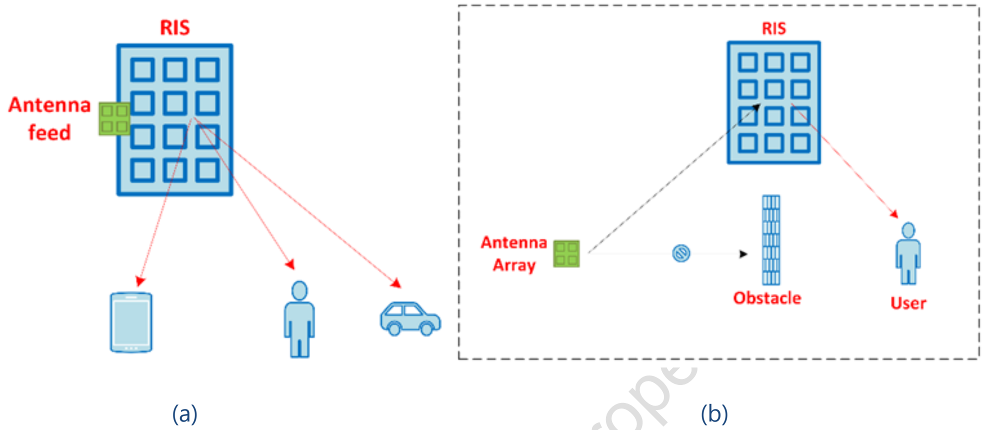

Figure 15. Reconfigurable intelligent surface use case scenarios, (a) RIS used as an intelligent reflector, (b) RIS used to reconfigure signal paths around obstacles (e.g. in a factory environment).

5.2. TMA/FMA/FD-RFIC

5.2.1. Full Duplex Use Cases

The Full Duplex functionality can potentially support communication, sensing and timing synchronization in different use cases, with different isolation requirements as KPI. The quantitative evaluation of those specifications will be carried out in a second step but in this document, as a first step, we will identify the specific use cases for which In-Band Full Duplex is considered and discuss the rationale for self-interference rejection.

- Radar Sensing

In the radar mode, the Tx and Rx are operating simultaneously. The self-interference between Tx and Rx will translate into range sidelobes which will degrade the sensitivity. Fortunately, after range processing, self-interference ends up mainly as a false-detection zero-range target. Minimizing receiver impairments in combination with an appropriate choice of the signal waveform can relax the self-interference cancellation requirements.

- Synchronization during Downlink Communication

Funded by
the European Union

While transmitting (half-duplex) information to the UE, the AP is expected to receive a synchronization signal from another AP. Even if another antenna panel or frequency is involved, the coupling of the transmitted signal might still affect the sensitivity of the synchronization loop. Therefore, a specification of Signal to Interference Ratio should be extracted for the specific synchronization solution to be developed.

- Synchronization during Uplink Communication

While receiving (half-duplex) communication from the UE, an Access Point may need to simultaneously transmit a synchronization signal to another Access Point. In that configuration, the coupling of the synchronization signal might degrade the sensitivity of the UE-receiver. A classical Signal to Noise ratio evaluation should be enough in that case.

- Full Duplex AP-AP Communication

For AP-AP links, the objective is to support simultaneous data distribution and gathering to a single fiber-access point via multiple hops. Therefore, the objective is to implement Full Duplex communication with wide bandwidth (potentially up to 400MHz) at high modulation level (256-QAM) to maximise data throughput. The most challenging isolation requirements likely come from this high sensitivity 256-QAM scenario. Fortunately, the static configuration of AP nodes likely helps, but we need to analyze and this in more detail and develop a test scenario for this case.

- TDD Operation

Different use-cases will be re-using the same hardware but in different time slots. Since the specifications may differ from case to case, we will consider reconfigurable hardware solutions. Reconfiguration can be applied at many levels in the system, but we will mainly consider it in the IC hardware, the antenna array and the choice of signal waveform.

5.2.2. Full Duplex Architecture

Many architectural possibilities are available to cancel the coupling between the transmitter to the receiver and it can be applied at any level of the signal chain. Figure 16 gives a description of a generic full duplex architecture where all possible cancelling loop are depicted. The green receive chain represents the main receive path, whereas the pink transmit chain is the main transmitter. An additional transmit chain labelled Tx_cancel can be exploited to cancel the coupling in the electromagnetic domain. An additional receive

Funded by the European Union

chain can also be exploited to measure and cancel the signal generated by the main transmit chain including distortion and noise impairments. In that case, the associated antenna can be replaced by a coupler. It should be noted that the number of receive paths n needs not be equal to the number of transmit paths m. These two variables can be adjusted to adapt to different full duplex use cases.

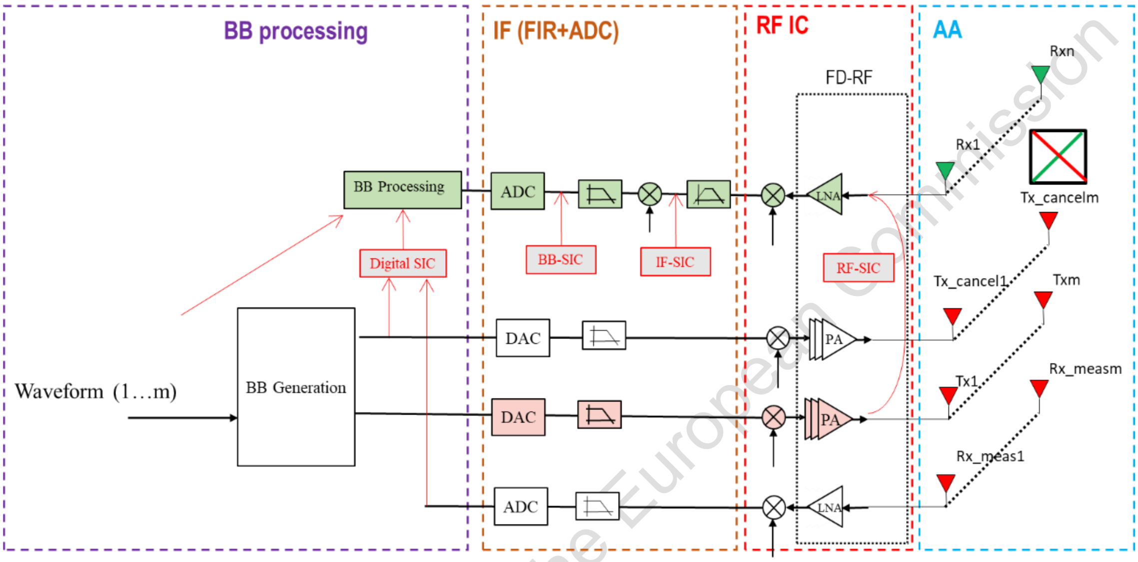

Figure 16. Complete Full Duplex Architecture

Self-Interference Cancelling (SIC) or attenuation can in principle be applied at all stages of the receive chain, e.g. in the antenna array and baseband processing, but also at the RF or IF stage. It is not the purpose of this document to enter in detail with the state of the art, but each domain has been studied in detail and some initial link budget estimates have been worked out. So far we didn't identify show-stoppers, but further detailed analysis will be carried out in the coming year considering feasibility but also cost and complexity.

Several degrees of freedom exist to improve the isolation and/or SIC. Antenna polarization is often used, but likely conflicts with direct use of orthogonal polarization as capacity doubler. The distance is a key factor to improve the isolation, as depicted in Figure 17, obtained by Jianfeng Qian and Yi Wang from Birmingham University.

Funded by the European Union

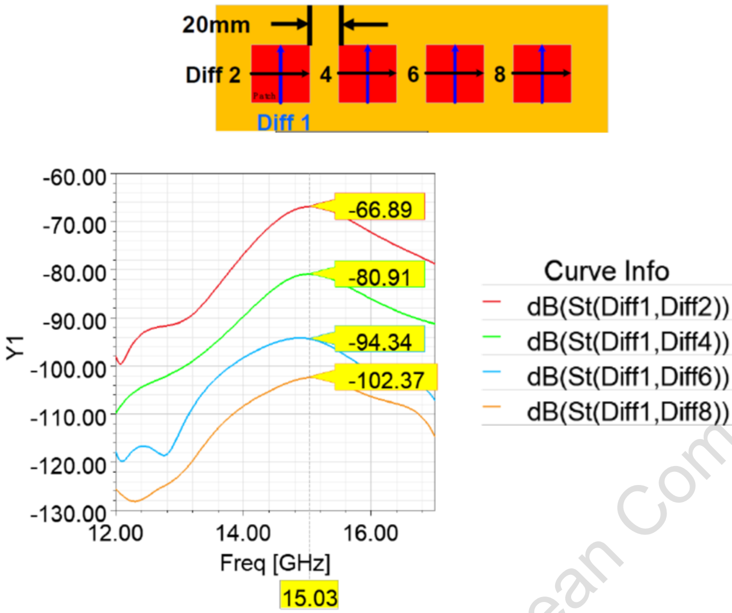

Figure 17. Influence of the distance on the antenna element isolation (Diff signals represent different signals across antenna patches with different polarizations (odd⇔vertical, even⇔horizontal))

The number of antenna elements in the array as well as their respective position is therefore also a key criterion. Specific materials or isolators can also be exploited. Some antenna elements can also be exploited to achieve some RF interference cancelling at the electromagnetic wave level. The overall size of the antenna panel is the cost to be paid when improving the isolation at the antenna level. Interference cancelling can also be implemented at the LNA (RF-SIC). It can be single- or multi-tap as a function of the targeted bandwidth and cancelling efficiency. This cancelling may degrade the receiver sensitivity because of additional noise. However, the main benefit is that it can avoid saturation of the LNA and it also gives an additional degree of freedom for the overall optimization. At the IF stage, more complex filtering can be implemented, especially with longer delay (IF-SIC). Moreover, baseband cancelling (BB-SIC) can be implemented to relax the ADC requirements and to avoid that ADC impairments increases the range sidelobes in radar mode. Finally, Digital Self-Interference Cancelling (Digital SIC) is undoubtedly indispensable for reaching high isolation. Lastly, especially for radar, waveform selection is also a key degree of freedom since it not only impacts the BB processing at the receiver side but also influences the coupling at the antenna array level. All these parameters will be considered to fulfil the specification listed in this document.

5.2.3. TMA/FMA Arrays and Their Efficiency Evaluations

TMA Transmitter and Receiver Arrays

In the D-MIMO architecture proposed in our 6G REFERENCE project, concurrent multi-beam capabilities are essential for several applications scenarios of communication and sensing. On the communication scenarios, several D-MIMO communication cases require one DU to simultaneously communicate with multiple fixed-position RUs (Figure 8 and Figure 10), so that the RUs can thus form high-quality D-MIMOs for UEs. These cases are needed for both urban and factory application scenarios. For the sensing and localization scenarios, it is highly desired to enhance the angular accuracy/resolution as well as enable sensing and tracking of multiple objects simultaneously.

Analog beamforming and hybrid beamforming architectures are scalable for large-element arrays but are challenging to support concurrent multi-beams without physically implementing multiple phase shifters and beamforming paths. Digital beamforming performs beam management at the digital backend and supports the best flexibility for concurrent multi-beam operations. However, they require high speed digital and mixed-signal circuits, whose complexity and power overhead may not be suitable for many low-cost applications. We propose to explore Time-Modulated Array (TMA) beamforming architectures in this 6G Reference project to address the concurrent multi-beam applications while ensuring minimum overhead on the circuit complexity, power, and operation of the arrays.

A TMA exploits timing modulations on the antenna elements to create time-varying array patterns as an orthogonal modulation added onto the existing beamforming patterns of the array. The time-varying patterns are often periodic and digital-like. On-off sequences and duty cycles can be designed to generate multiple concurrent beams with different features, such as different beam numbers, beam directions, beam strengths, and beam offset frequencies. Although TMAs are a popular concept among the antenna community, it is rarely explored with integrated electronics implementations and demonstration, creating opportunities for our research.

As our initial research, we focus on system specification and feasibility study to link the TMAs with envisioned 6G REFERENCE application scenarios. We have explored capabilities of multi-beam generation in communication and sensing use cases. As a first step, we evaluate the multi-beam generation capability of TMA TX array and compare it with standard phased array based beamformers in terms of the number of concurrent beams, and the resulting TX array gain and EIRP. The results are shown in Figure 18 with six TX architectures in comparison: (1) a standard N-element single-beam beamformer, (2) an N-element analog beamformer with M sub-arrays, (3) a fully-connected N-element (analog or digital) M-beam beamformer, (4) an N-element TMA with amplitude-modulation (AM) scheme, (5) an N-element TMA with phase-modulation (PM scheme), and a proposed architecture which consists of a $M \times M$ Butler Matrix cascaded with an N-element TMA with PM scheme. For this comparison, we make the following assumptions: (1) the continuously-ON TX array element average power consumption is PDC (in dBm), (2) the continuously-ON TX array element is capable of generating a maximum linear average output power of $Pout$ (in dBm), (3) the PA dominates the TX DC power consumption, and (4) the peak-to-average power ratio (PAPR) of the data streams is neglected for simplicity.

Case-1: For the standard N-element single-beam beamformer, there is an array gain of 10log N (in dB) and another enhancement in the EIRP of 10log N (in dB) due to the addition of the output power of N PAs that are always ON. Therefore, the beam EIRP (in dBm) is $Pout$ + 20log N, while the TX array average power consumption (in dBm) is PDC + 10log N. Accordingly, the TX array efficiency, defined as the TX aggregated EIRP divided by the total TX array average power consumption can be calculated (in dB) as $Pout$ - PDC + 10log N.

Case-2: For the N-element analog beamformer with M sub-arrays, which involves dividing the entire array to M sub-arrays each transmitting one independent beam, the TX aggregated EIRP (in dBm) and the array efficiency (in dB) will degrade by a factor of 10log M, compared to the single-beam beamformer case, because the entire array aperture is not utilized for all the beams.

Case-3: On the other hand, a fully connected N-element array with M concurrent beams can do better. By utilizing the whole array aperture in the fully connected (digital or analog) M-beam beamformer, the TX array can achieve the same aggregated EIRP and the same array efficiency as the single-beam beamformer, while producing M independent beams. It is worth noting that the 10log M reduction in the EIRP per beam for the fully connected scenario is due to the conservation of energy, i.e., the average output power of each PA ($Pout$) needs to be split among the M independent streams it processes.

Case-4: For an N-element TMA with AM scheme, a concurrent N+1 beams are produced with an approximate gain of 0dB per beam. Further, given that only one PA is turned ON,

Funded by the European Union

on average, during operation due to the duty-cycled ON/OFF scheme of TMA with AM, the TX aggregated EIRP (in dBm) is only enhanced by 10log N (in dB) and is found to be $Pout$ + 10log N. However, at the same time, due to the duty-cycled ON/OFF operation, the total TX array average power consumption (in dBm) is now equal to the average power consumption of a single continuously-ON PA, which is PDC. Therefore, the TX array efficiency is preserved and is similar to that of the single-beam beamformer and the fully connected M-beam beamformer.

Case-5: Moving from the TMA with AM scheme to PM scheme, a further 10log N enhancement in the aggregated EIRP can be achieved due to the fact that the N PAs are always turned ON, resulting in the same aggregated EIRP and the same array efficiency as the fully-connected M-beam beamformer.

Case-6: For the proposed multi-beam TX architecture, which cascades an $M \times M$ Butler matrix with an N element TMA, a larger number of concurrent beams, which is equal to $M\times(N+1)$, can be generated, with a reduced EIRP per beam (in dBm) of 10log (N/M). However, when assumming for all the beams, the aggregated EIRP and TX efficiency are found to be similar to that of the fully-connected M-beam beamformer.

In summary, there is a fundamental trade-off between the number of concurrent beams and the EIRP per beam in all beamforming architectures. One virtue of the proposed TMA based multi-beam TX beamformer architecture is the ability of concurrently generating multiple-beams with low hardware complexity, while maintaining the same aggregated TX EIRP and array efficiency as fully-connected beamformers, i.e., conservation of aggregated TX EIRP and array efficiency regardless of the number of concurrent beams, which is highly desired for our 6G REFERENCE applications. In comparison, although duplicating hardware to realize parallel analog beamformers renders the most flexible independent beam steering capabilities, this approach is difficult to scale for a large number of beams. As our next research steps, we will further explore the TMA TX architectures and operations to best match the D-MIMO application scenarios.

Since the TMA operation is both linear and reciprocal, it is conceived that the same beamforming properties hold true also for TMA RX arrays. However, concerning the TMA RX arrays, additional requirements on array SNR for all the noise scenarios (in-/out-band noise and source/array noise), array linearity, downstream IF bandwidth, and ADC speed and resolution deserve further investigations. As our next steps, we will explore these TMA RX array system properties and trade-offs to meet the D-MIMO applications in our 6G REFERENCE project.

Funded by the European Union

Finally, it should be clarified that the TMA TX or RX operations are essentially "add-on" operations on the analog or hybrid beamforming TX or RX arrays. Therefore, they do not have additional requirements on the frontend RF circuits specifications of these arrays. On the other hand, to ensure proper TMA operations, high-quality time-modulation clocks at sufficient speed are needed. First, the TMA clock speed should be higher than the RF bandwidth, or twice of the baseband bandwidth, of the modulation, to meet the Nyquist criteria. In the 6G REFERENCE project, since the maximum modulation bandwidth is 400MHz, with sufficient margin, we target the TMA clock speed as 500MHz or above, which can be supported by advanced CMOS or CMOS SOI technologies, such as Globalfoundries 22FDX. Secondly, the TMA clock rising and fall time should be sufficiently sharp to ensure TMA beam quality and signal fidelity. In practice, this rising and fall time should be less-than 10% of the total TMA clock period,

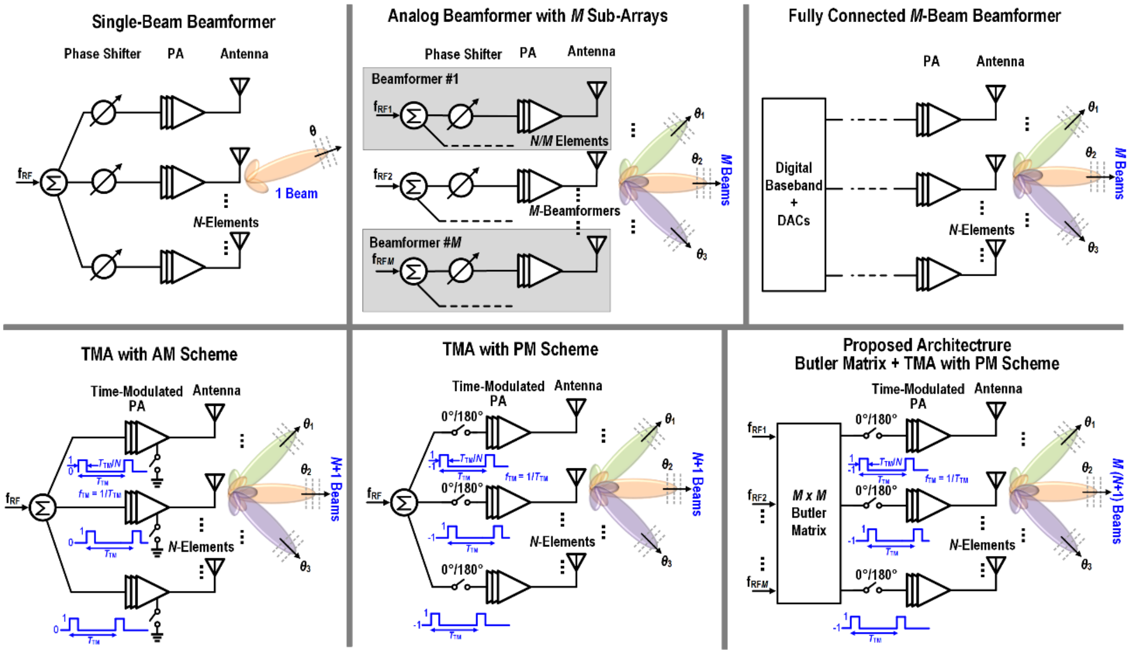

	Single-Beam Beamformer	Analog Beamformer with M Sub-Arrays	Fully-Connected M-Beam Beamformer	TMA with AM Scheme	TMA with PM Scheme	Proposed Arch. (Butler Matrix + TMA with PM Scheme)
Number of Elements	N	N	N	N	N	$M \times M$ Butler Matrix $+ N$-Element TMA
Number of Concurrent Beams	1	M	M	$N+1$	$N+1$	$M \times (N+1)$
Array Gain per Beam (dB)	$10 \log N$	$10 \log (N/M)$	$10 \log N$	~0	~0	~0
Time-Averaged Number of ON Elements per Beam (dB)	$10 \log N$	$10 \log (N/M)$	$10 \log N$	0	$10 \log N$	$10 \log N$
EIRP per Beam (dBm)	$P_{out} + 20 \log N$	$P_{out} + 20 \log N - 20 \log M$	$P_{out} + 20 \log N - 10 \log M$	P_{out}	$P_{out} + 10 \log N$	$P_{out} + 10 \log N - 10 \log M$
TX Aggregated EIRP (dBm)	$P_{out} + 20 \log N$	$P_{out} + 20 \log N - 10 \log M$	$P_{out} + 20 \log N$	$P_{out} + 10 \log N$	$P_{out} + 20 \log N$	$P_{out} + 20 \log N$
TX Array Average Power Consumption (dBm)	$P_{DC} + 10 \log N$	$P_{DC} + 10 \log N$	$P_{DC} + 10 \log N$	P_{DC}	$P_{DC} + 10 \log N$	$P_{DC} + 10 \log N$
TX Array Efficiency (dB) (Total EIRP / Total Power Cons.)	$P_{out} - P_{DC} + 10 \log N$	$P_{out} - P_{DC} + 10 \log (N/M)$	$P_{out} - P_{DC} + 10 \log N$	$P_{out} - P_{DC} + 10 \log N$	$P_{out} - P_{DC} + 10 \log N$	$P_{out} - P_{DC} + 10 \log N$

Figure 18. A comparison between the proposed TMA-based concurrent multi-beam TX architectures with single-beam and multi-beam fully-connected sub-array-based beamformers in terms of number of concurrent beams, gain, EIRP and efficiency.

Frequency Modulated Array (FMA)

For the sensing applications of our 6G REFERENCE project, it is essential to localize and detect objects in a fast and high-precision manner. In addition to the proposed FMCW radar and MIMO radar schemes, we also aim to explore the Frequency Modulated Array (FMA) architectures, which is a combination of time modulation and the Frequency Diversity Array (FDA) architectures in the radar community. In essence, the FMA/FDA uses incremental frequency offsets across its elements, enabling beam steering through time-dependent phase shifts in both angular and range domains. This automatic beam scanning and range-awareness set the FDA apart from conventional Phased Arrays, highlighting its potentials in next-generation joint sensing and communications systems.

The standard FDA utilizes linearly incremental frequency offsets to produce an S-shaped periodic beampattern that varies with both range and angle. Figure 19 demonstrates these beampatterns for a typical 8-element standard FDA operating at 20GHz with 50MHz frequency increments. Contrasting with the range-agnostic Phased Array, the FDA automatically scans both range and angle over time.

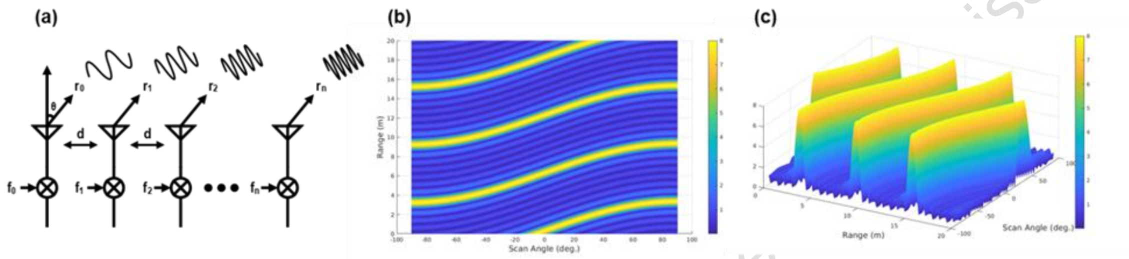

Figure 19. (a) Schematics of a uniform linear FDA array. (b) and (c) Beampattern of a standard FDA with linear frequency offset.

However, the inherent ambiguity in the coupled range-angle beampatterns of Frequency Diverse Arrays (FDAs) complicates target localization. Traditional FDAs are limited in their ability to localize receivers (RXs) accurately, as they necessitate the sequential determination of either range or angle. This sequential approach poses a challenge, as both parameters are typically unknown in practical scenarios and need to be concurrently resolved for effective localization.

Therefore, in our 6G REFERENCE, we see to explore methods that decouple FDA beampatterns in range and angle dimensions and are compatible with practical integrated electronics implementations. Possible techniques involve using nonlinear frequency offsets. Figure 20 demonstrates how applying a Hamming window to the frequency offsets for each element yields a range-angle-decoupled "dot" shaped beampattern. This configuration allows for scanning across the range over time while maintaining a constant angle, which can be further steered as the conventional phased array.

Funded by the European Union

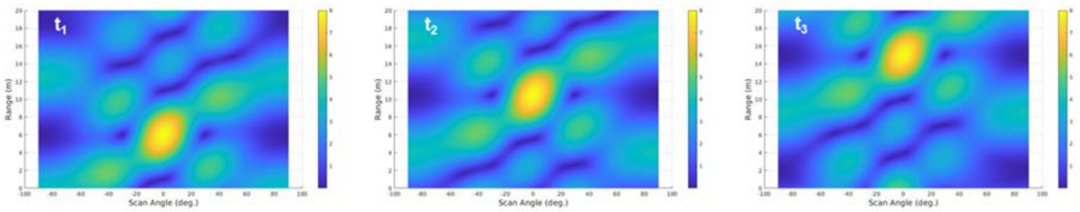

Figure 20. Beampattern of an FDA employing Hamming windowing on frequency offsets, depicted at three different time instances.

Some other non-linear frequency offset methods, such as square, cubic, logarithmic, and piecewise trigonometric offsets, provide diverse "dot-shaped" beampattern options. In addition, utilizing multi-carriers for a single element and combined with a convex optimization algorithm allows for the creation of sharp "multi-dots" beampatterns. These advanced non-linear techniques necessitate careful consideration of the trade-offs between the complexity of implementation, main-beam width, and sidelobe suppression. Figure 21 illustrates several examples of these range-angle-decoupled "dot" shaped beampatterns demonstrated in the literature.

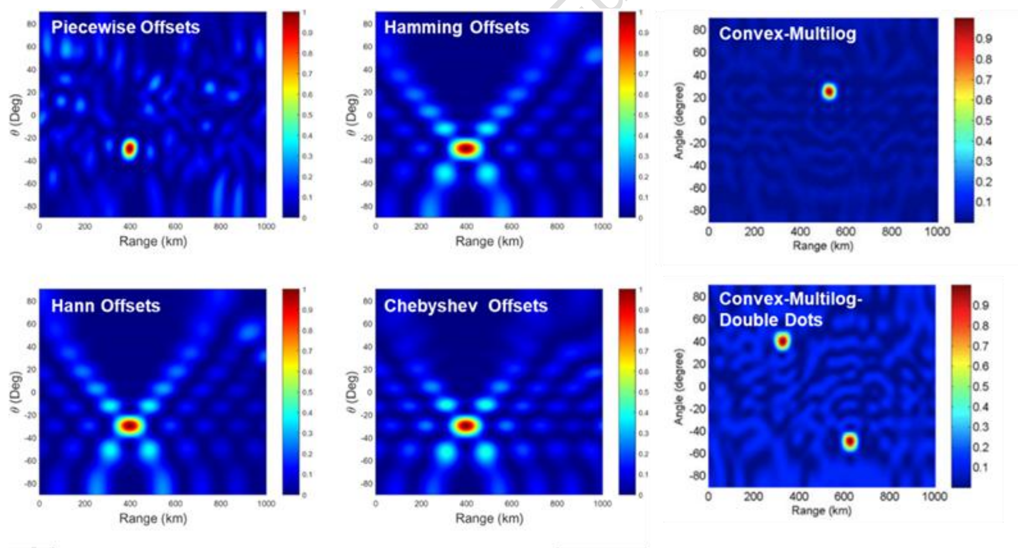

Figure 21. Beampattern of FDA with various nonlinear frequency offsets.

While nonlinear frequency offsets effectively decouple FDA beampatterns into range and angle dimensions, the resulting patterns remain time-variant. Efforts to eliminate this time periodicity using time-modulated nonlinear frequency offsets aim to enable static point-to-point communication. However, these attempts have largely remained theoretical and are challenging to validate due to subtle mathematical nuances.

Recent research has identified inherent limitations in time-invariant FDA approaches, confirming that FDA beampatterns inevitably exhibit time variance due to the previously overlooked propagation effects. Despite these setbacks, significant research potential exists in integrating FMA with TMA for advanced applications in communication and sensing. This integration can leverage the inherent time variance, rather than attempting to eliminate it, as illustrated in the following example.

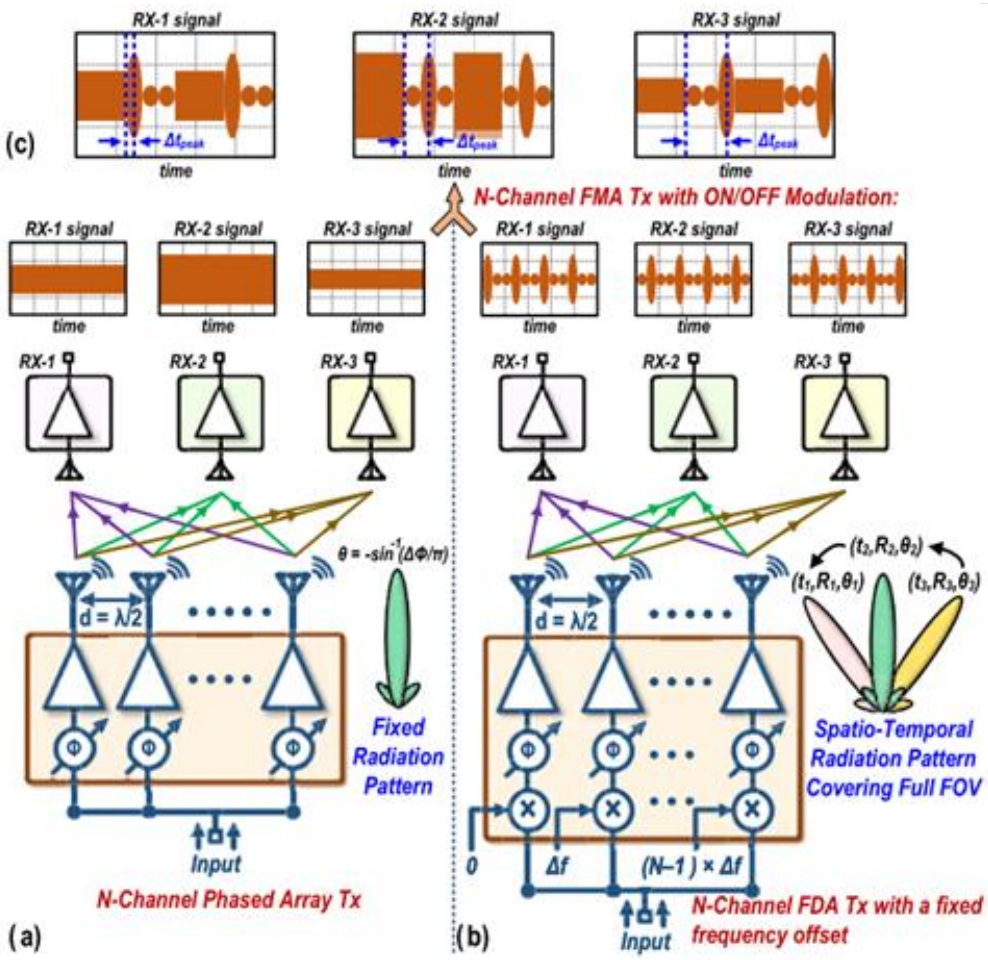

Figure 22. (a) Conventional phased array (b) FMA as FDA combined with time varying radiation pattern (c) ON/OFF FMA operation for RX localization

Figure 22 illustrates an FMA array architecture employing time-domain ON/OFF modulation on the frequency offset of FDA array. Initially, the FMA array operates in conventional phased array mode to establish a timing reference. Then, the transmit (TX) array switches to ON mode, activating FDA mode and leveraging the spatial-temporal beampattern for automatic full field of view (FoV) scanning. At the receive (RX) nodes, the peak of the time-varying pattern occurs at different times for various angular locations. The time difference between this peak and the timing reference (Δt_{peak}) offers a unique angular solution, aiding in RX localization.

The relationship between the angle and the timing difference enables us to solve for the angle when the time difference is known, providing a unique solution. This FMA scheme is antenna-agnostic and only requires a modest megahertz (MHz) frequency offset for mm-Wave carriers to achieve super-resolution localization. For instance, with a frequency offset of 2MHz, the four-element FMA array achieves an angular resolution of 2° with a relaxed timing discrimination of 10ns in timing difference, confirming its capability for super-resolution Tx/Rx localization. Notably, this represents a Lidar-grade angular resolution, typically achievable only with large phased arrays containing tens to hundreds of elements. Furthermore, the angular resolution can be further improved by using a smaller frequency offset, as the timing difference is inversely proportional to frequency offsets.

In practice, aside from the practical challenges of synthesizing a small frequency offset, careful trade-offs must be considered regarding the minimum sensing time when selecting frequency offset. When the FMA mode is activated, it is crucial to design sufficient cycles of the sinc-like radiation pattern to ensure that a peak is detected. Since the periodicity of the peak in the sinc-like pattern is inversely proportional to frequency offset, using a very small frequency offset will require a longer minimum sensing time. Therefore, balancing the benefits of a smaller frequency offset with the associated increase in sensing time is crucial for overall system performance, particularly in joint sensing and communication applications, where only a portion of the symbol duration can be allocated to sensing. This careful trade-off ensures that both sensing resolution and communication data rate are optimized. Additionally, such approach is readily compatible with standard FMCW (Frequency Modulated Continuous Waveform) radar for enhanced depth resolution. Finally, just like TMAs, the FMAs are also "add-on" functions on standard analog/hybrid beamforming arrays, and thus there is no additional specification requirements on the RF chains for FMA TX and RX arrays. However, the frequency/time modulation signals of FMAs will be judiciously designed to meet the application scenario specifications. For instance, for our proposed 6G REFERENCE joint communication/sensing arrays, the target sensing slot is 16.7us-8.3us to fit within one single OFDM symbol (corresponding to subcarrier spacing of 60kHz/120kHz respectively). This translates to minimum frequency modulation offset frequency of 1MHz with margin to complete the FMA signal acquisition, which can be readily implemented by advanced CMOS/CMOS SOI technologies, such as Globalfoundries 22FDX. In summary, all these practical design aspects will be explored in the research tasks in the 6G REFERENCE project.

5.3. RF-SYNC-IC / RFXO-PLL

The timing specifications can be split into two parts, namely specifications for short-term accuracy (e.g. jitter and phase noise), and long-term accuracy (e.g. frequency synchronization tolerance). The short-term accuracy is achieved by the RFXO-IC block, usually by a high-Q LC oscillator. This block is tuned by a second block, the RF-SYN-IC, which is responsible for the long-term frequency and time synchronization. A block overview is shown in Figure 23.

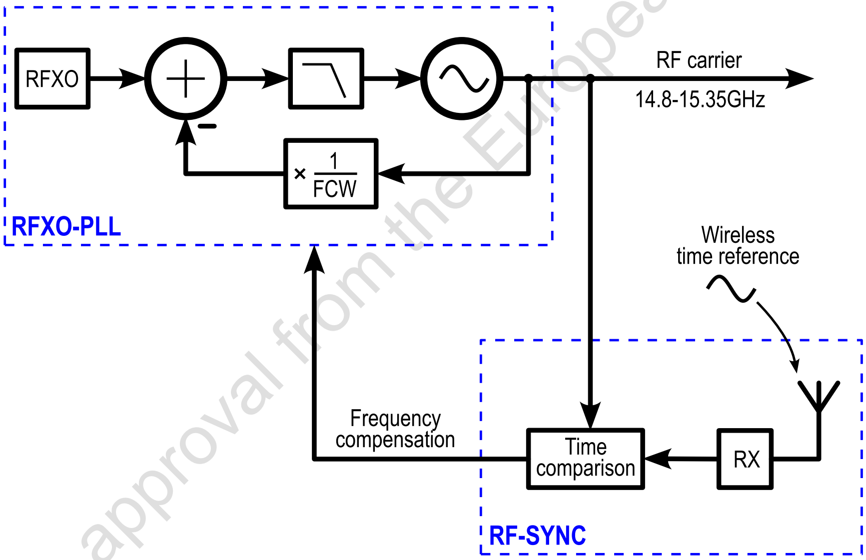

Figure 23. Time synchronization block overviews.

5.3.1. RFXO-PLL

The RFXO-IC blocks synthesizes the RF carrier used in the transmitter and receiver. The frequency of the carrier is in the range of 14.8GHz to 15.35GHz (in case of zero-IF, or shifted when nonzero-IF is used). The main requirement for this block to achieve a jitter less than 100fs, as stated in Section 4.4.

In order achieve this jitter specification, we will use a high-frequency, low phase noise reference in conjunction with a high PLL bandwidth. A disadvantage of these high frequency references is that these usually come with a poor absolute frequency accuracy and poor temperature stability. In order to achieve a stable, accurate RF frequency, OTA frequency synchronization will be employed.

5.3.2. RF-SYNC-IC

The total time offset $\Delta T(\tau)$ of a frequency synthesizer with respect to absolute time τ can be modeled as (Riley, 2008):

$$\Delta T(\tau) = T_0 + \frac{\Delta \mathrm{f}}{\mathrm{f}}\tau + \frac{1}{2}D\tau^2 + \sigma_x(\tau),$$

where T_0 is the initial time offset, $\frac{\Delta f}{f}$ is the fractional frequency offset, D is the frequency drift and $\sigma_x(\tau)$ is the TDEV. Assuming that frequency aging is not dominant, the most dominant error sources are the fractional frequency offset $\frac{\Delta f}{f}$ and the TDEV $\sigma_x(\tau)$.

A larger synchronization interval τ results in a bigger time offset, as the frequency offset component is proportional to τ and the TDEV generally increases for larger τ. Therefore, a tradeoff exists between synchronization interval and time error. Faster synchronization relaxes the TDEV and frequency offset requirement, while a slower synchronization reduces the resources (bandwidth, SNR) needed for synchronization.

Our targeted maximum acceptable time error is ±4ps to allow D-MIMO. Assuming a synchronization interval of 1 millisecond, the fractional frequency error must be smaller than 4ppb, which is in the same order of magnitude as the sensing requirement described in Section4.4. Hence we conclude that TDEV of the local oscillator must be smaller than 4ps within the synchronization interval.

5.4. IF-ADC IC

The IF-ADC can support zero-IF and a higher IF-frequency. In case of non-zero IF, the IF signals will be downconverter to baseband frequencies and converted to digital by an A/D converters. The target ADC resolution of 12 bits and sample rate of about 250 MS/S is chosen to cover 100MHz with some oversampling, while staying in the energy efficient region of the Murmann plots (Murmann 2024). Instead of pushing for higher sampling rates for signal bandwidths wider than 100MHz, we plan to implement multiple slices of the IF demodulator, convert adjacent stripes in parallel and combine the results, if necessary, digitally.

To mitigate dynamic range requirements of the ADC, variable gain amplifiers and baseband filters will be implemented, to remove large out of band blocking signals and adjust the signals to the optimum level required by the ADC input for best performance.

Depending on the system frequency planning to optimise the overall performance, the IF demodulator will support a range of IF frequencies, ranging from 1GHz to 6GHz. To facilitate RF filtering the IF frequency should not be less than 1/10 of the RF frequency so that required RF filter quality factor will not exceed 10. For FR3 signal bands this will mean 1.5GHz IF frequency will be sufficient. We aim to provide support for higher IF frequencies, to lessen RF filter requirement even further. Higher IF also has the additional benefit that it may allow the RF local oscillator frequency to be lower, hence consuming less power and achieving better performance. For example, if the RF frequency is at 15GHz and IF frequency is set to be 6GHz, then the LO frequency only needs to be 9GHz, instead of 13.5GHz if the IF is at 1.5GHz. The quadratic relationship between oscillator frequency and current consumption can be saving half the power.

5.5. FIR-IF IC

To support the TMA receiver concept that maps different beam directions to different IF-frequencies and to realize flexible IF-filtering supporting multiple bandwidths and IF-frequencies, we propose an FIR-IF filtering including downconversion based on an extension of a technique known as "Filtering by Aliasing". It can provide a flexible digitally programmable frequency downconversion which allows to combine the mixer and the IF-filter shown in Figure 9 in one block (see Figure 24), while reducing ADC dynamic range requirements.

Funded by the European Union

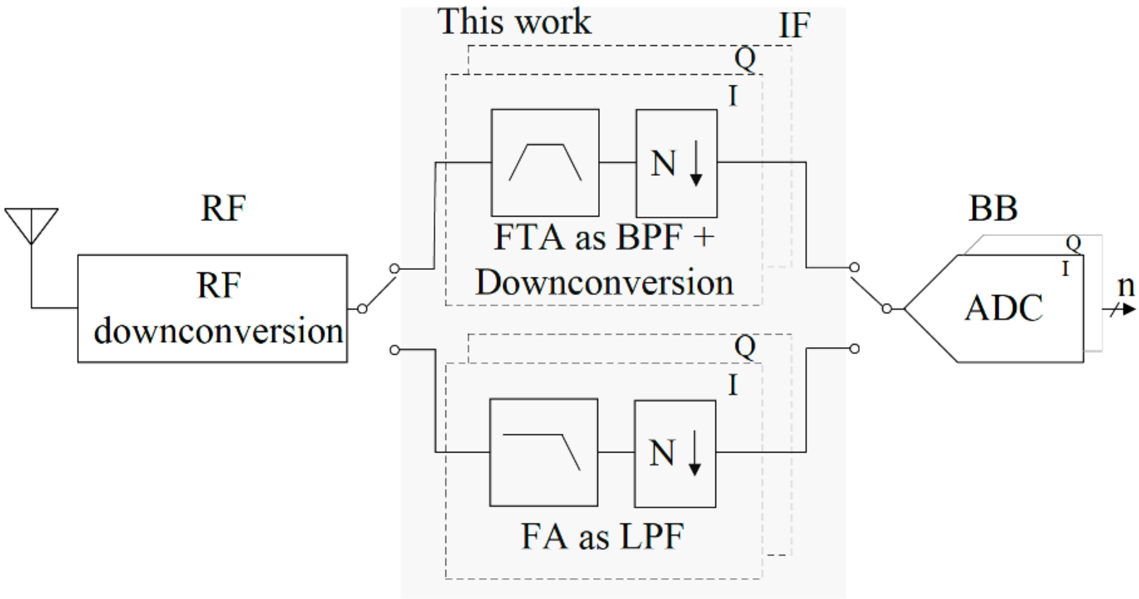

Figure 24. Proposed IF architecture integrated with a RF downconversion at its input and IQ ADCs at its output.

We aim to explore an implementation with a time-varying gm supporting the RF system bandwidths of 50, 100, 200 and 400MHz. The filter should support zero-IF functionality but at the same time allow to support concurrent TMA IF channels. Assuming that the individual channel bandwidth is 50-400MHz and the TMA spacing between the concurrent IF bands is >400MHz to avoid in-band alias bands, the FIR-filter will need to run approximately at 2GS/s sample rate to support 4 simultaneous beams. We will also explore alias-suppression techniques so that the output of the FIR filter can be directly sampled by the ADC without aliasing limiting the dynamic range. Additional upfront alias suppression with a passive-LC filter will be explored in combination with this FA-IF architecture.

5.6. XC-PRS Algorithms and Hardware Accelerators

We performed some initial system study accurate and robust over-the-air time-synchronization (OAS) with pseudo-random sequences (PRS). Simple correlation techniques, as for instance used in receivers for global navigation satellite systems (GNSS), turn out to be insufficient in the considered scenarios defined in chapter 2. In fact, the presence of significant multipath components (which are absent in typical GNSS-to-Earth outdoor links, but present indoors) inevitably result in timing-estimation errors. For example, a dominant propagation path only 10m longer than another path, already induces a timing uncertainty of 33.4ns, which spreads the peaks of a simple correlation procedure with the PRS over multiple samples, even for systems with moderate bandwidths. Since (i) one cannot easily distinguish which correlation peak corresponds to the shortest path (especially under non-LoS conditions) and (ii) an early LoS path may not be detectable due to fading, improved correlation algorithms (XC) are necessary. To address this limitation, we aim to develop novel multipath-aware correlation algorithms (XC-PRS, for short). Concretely, we plan to develop methods that jointly estimate the channel's impulse response (which is possible as the PRS is known at the receiver) and the most likely delay, inspired by a method put forward in (de Filomeno M. L., *et al.* 2022). We think this is possible under the assumption that we know the maximum delay spread of the dominant paths which will be determined by the scenario. The result of such a multipath-aware correlation procedure will enable one to discover earlier but less significant correlation peaks, which, in turn, is expected to result in improved timing estimates. In addition, we will pursue the use of nonlinear denoising techniques (based on a-priori knowledge of the channel statistics), which are expected to further improve resilience. Finally, based on the outputs of the refined correlation algorithm, we will estimate the carrier frequency offset (CFO) between transmitter and receiver as in (Schmidl and Cox, 1997).

While promising improved accuracy in multipath environments, we expect such XC-PRS correlation algorithms to result in at least one order-of-magnitude higher computational complexity when compared to naïve correlation. Thus, practical systems inevitably require specialized hardware accelerators that are (i) able to process the received I/Q baseband data stream at several million samples per second (determined by the target bandwidth) while (ii) being energy and area efficient. We will develop such accelerators on register-transfer level (RTL) that support the targeted bandwidths of up to 400MHz and fabricate a prototype of the most promising solution in GF 22FDX.

6. Conclusions

This report summarizes initial system study work done in the 6G-Reference project to convert rather general ideas on useful hardware capabilities/enablers for future 6G systems to concrete system and block level KPIs for concrete use-case scenarios. We evaluated various proposed 6G use-case scenarios related to communication and sensing, with special focus on HEXA-XII. We selected three best fitting use cases: 1) An urban square communication scenario with densely distributed RUs, enhanced with basic sensing capabilities; 2) A factory hall scenario with more a regular deployment grid supporting communication but also higher performance sensing capabilities; 3) A timing focussed scenario (Time Sensitive Network) with special focus on providing high performance time stamping to UTC. We selected the 14.8-15.35GHz cm-wave band as target band with 50-400MHz channel bandwidth and defined a deployment grid with about 25m spacing between access points. Requirements on communication and sensing were defined in quite some detail linked to the use-case scenarios. Moreover, initial key KPIs for the blocks were identified and some initial system level feasibility estimates were made.

In the coming period we will work out these block requirements in more detail and explore the design space for the building blocks and performance feasibility.

References

3GPP (2024a) '3GPP Stage-1 Workshop on IMT2030 Use Cases'. Available at: https://www.3gpp.org/technologies/stage1-imt2030-uc-ws (Accessed: 12 August 2024).

3GPP (2024b) '3GPP TS 38.104: Technical Specification Group Radio Access Network, NR, Base Station (BS) radio transmission and reception (Release 18)'. Available at: https://www.3gpp.org/ftp/Specs/archive/38_series/38.104/38104-i50.zip.

3GPP (2024c) '3GPP TR 22.837: Technical Specification Group Radio Access Network, SA: Feasibility Study on Integrated Sensing and Communication (Release 19)'. Available at: https://www.3gpp.org/ftp/Specs/archive/22_series/22.837/22837-j40.zip.

5G-ACIA (2023) *Integration of 5G with Time-Sensitive Networking for Industrial Communications*, *5G-ACIA*. Available at: https://5g-acia.org/whitepapers/integration-of-

Ammar, H. A., Adve, R., Shahbazpanahi, S., Boudreau, G., & Srinivas, K. (2022). Downlink Resource Allocation in Multiuser Cell-Free MIMO Networks With User-Centric Clustering. *IEEE Transactions on Wireless Communications, 21*(3).

A. Bourdoux, R. Feng and M. Bauduin (2024), "Low PAPR Design for OFDM Symbols with Guard Bands and Baseband Filtering," 2024 IEEE Radar Conference (RadarConf24), Denver, CO, USA, 2024, pp. 1-6, doi: 10.1109/RadarConf2458775.2024.10548775.

Bogdanov, P. *et al.* (2018) 'Analysis of GNSS time scales', in *2018 European Frequency and Time Forum (EFTF). 2018 European Frequency and Time Forum (EFTF)*, Turin: IEEE, pp. 181–184. Available at: https://doi.org/10.1109/EFTF.2018.8409027.

de Filomeno M. L., *et al.* (2022), `Joint channel estimation and Schmidl & Cox synchronization for OCDM-based systems,' in IEEE Communications Letters, vol. 30, no. 26, pp. 1878-1882, May 2022, https://doi.org/10.1109/LCOMM.2022.3178865

Di Renzo *et al* (2020) "Smart Radio Environments Empowered by Reconfigurable Intelligent Surfaces: How It Works, State of Research, and The Road Ahead," in *IEEE Journal on Selected Areas in Communications*, vol. 38, no. 11, pp. 2450-2525.

Eidson, J. (2005) 'IEEE-1588 Standard for a Precision Clock Synchronization Protocol for Networked Measurement and Control Systems'. Available at: https://www.nist.gov/system/files/documents/el/isd/ieee/tutorial-basic.pdf.

Hexa-X-II (2023) 'Hexa-X-UU Deliverable D1.2: 6G Use Cases and Requirements'. Available at: https://hexa-x-ii.eu/wp-content/uploads/2024/01/Hexa-X-II_D1.2.pdf (Accessed: 12 August 2024).

Interdonato, G. *et al.* (2019) 'Ubiquitous cell-free Massive MIMO communications', *EURASIP Journal on Wireless Communications and Networking*, 2019(1), p. 197. Available at: https://doi.org/10.1186/s13638-019-1507-0.

ITU (2023) 'Recommendation ITU-R M.2160-0 (11/2023) - Framework and overall objectives of the future development of IMT for 2030 and beyond'.

Lin, P. and Haliloglu, O. (2022) 'Layer-1 Mobility in Distributed MIMO with Non-Coherent Joint Transmission', in *2022 IEEE 96th Vehicular Technology Conference (VTC2022-Fall). 2022 IEEE 96th Vehicular Technology Conference (VTC2022-Fall)*, pp. 1–5. Available at: https://doi.org/10.1109/VTC2022-Fall57202.2022.10012990.

Madhow, U. *et al.* (2014) 'Distributed massive MIMO: Algorithms, architectures and concept systems', in *2014 Information Theory and Applications Workshop (ITA). 2014 Information Theory and Applications Workshop (ITA)*, pp. 1–7. Available at: https://doi.org/10.1109/ITA.2014.6804225.

Mahmood, A. *et al.* (2017) 'Clock Synchronization Over IEEE 802.11—A Survey of Methodologies and Protocols', *IEEE Transactions on Industrial Informatics*, 13(2), pp. 907–922. Available at: https://doi.org/10.1109/TII.2016.2629669.

B. Murmann (2024), "ADC Performance Survey 1997-2024," [Online]. Available: https://github.com/bmurmann/ADC-survey.

NGMN (2022) '6G Use cases and analysis'. Available at: https://www.ngmn.org/wp-content/uploads/220222-NGMN-6G-Use-Cases-and-Analysis-1.pdf (Accessed: 12 August 2024).

Ngo, H.Q. *et al.* (2017) 'Cell-Free Massive MIMO Versus Small Cells', *IEEE Transactions on Wireless Communications*, 16(3), pp. 1834–1850. Available at: https://doi.org/10.1109/TWC.2017.2655515.

Riley, W.J. (2008) 'Handbook of Frequency Stability Analysis', *NIST Special Publication 1065* [Preprint], (1065). Available at: https://doi.org/10.6028/NIST.SP.1065.

Ruffini, S. *et al.* (2021) '5G synchronization requirements and solutions', *Ericsson Technology Review*, 2021(1), pp. 2–13. Available at: https://doi.org/10.23919/ETR.2021.9904655.

Schmidl T. M., Cox D.C (1997). `Robust frequency and timing synchronization for OFDM.' in *IEEE Transactions on Communications,* vol.45, no. 12, pp. 1613-1621, Dec. 1997, https://doi.org/10.1109/26.650240

Yngvesson, K.S. *et al.* (1988). 'Realizable feed-element patterns and optimum aperture efficiency in multibeam antenna systems', *IEEE Transactions on Antennas and Propagation*, vol. 36, no. 11, pp. 1637-1641, Nov. 1988, doi: 10.1109/8.9719

Vuyyuru S. K. R., *et al.* (2023), ´Efficient Anomalous Reflector Design Using Array Antenna Scattering Synthesis´ in *IEEE Antennas and Wireless Propagation Letters*, vol. 22, no. 7, pp. 1711-1715, July 2023, doi: 10.1109/LAWP.2023.3260920.